Inhibition of c-Jun in AgRP neurons mediates chronic stress-induced anxiety-like behaviors and colitis susceptibility

Fuxin Jiao[2], Xiaoming Hu[1], Hanrui Yin[2], Feixiang Yuan[1], Ziheng Zhou[2], Wei Wu[3], Shanghai Chen[1], Zhanju Liu[3,*], Feifan Guo[1,*]

[1]Zhongshan Hospital, State Key Laboratory of Medical Neurobiology, Institute for Translational Brain Research, MOE Frontiers Center for Brain Science, Fudan University, Shanghai 200032, China.

[2]CAS Key Laboratory of Nutrition, Metabolism and Food Safety, Innovation Center for Intervention of Chronic Disease and Promotion of Health, Shanghai Institute of Nutrition and Health, University of Chinese Academy of Sciences, Chinese Academy of Sciences, Shanghai 200031, China.

[3]Department of Gastroenterology, The Shanghai Tenth People's Hospital, Tongji University, Shanghai 200072, China

*Correspondence: Feifan Guo, PhD, Zhongshan Hospital, State Key Laboratory of Medical Neurobiology, Institute for Translational Brain Research, MOE Frontiers Center for Brain Science, Fudan University, Shanghai 200032, China. e-mail: ffguo@fudan.edu.cn; fax: +86-21-54237683. Zhanju Liu, MD, PhD, Department of Gastroenterology, The Shanghai Tenth People's Hospital, Tongji University, Shanghai 200072, China. e-mail: liuzhanju88@126.com; fax: +86-21-66303983.

ABSTRACT

Psychiatric disorders, such as anxiety, are frequently associated with inflammatory bowel diseases (IBD), however, the neural mechanisms are unknown. Here, we showed that hypothalamic agouti-related protein (AgRP) neuronal activity was suppressed under chronic restraint stress (CRS), a condition known to induce anxiety-like behaviors and increase colitis susceptibility. Consistently, chemogenic activation (inhibition) of AgRP neurons reversed (mimicked) CRS-induced anxiety-like behaviors and colitis susceptibility. Furthermore, CRS inhibited AgRP neuronal activity by suppressing the expression of c-Jun. As expected, overexpression of c-Jun in these neurons protected against the CRS-induced these effects and knockdown of c-Jun in AgRP neurons (*c-Jun*$^{\Delta AgRP}$) promoted anxiety-like behaviors and colitis. Moreover, relieving the anxiety with cyamemazine (an anxiolytic drug) alleviated colitis susceptibility in *c-Jun*$^{\Delta AgRP}$ mice. Finally, according to a proteomic analysis, the levels of the secreted protein thrombospondin 1 (THBS1) were negatively associated with the increased anxiety-like behaviors and colitis susceptibility, supplementing recombinant THBS1 rescued colitis in *c-Jun*$^{\Delta AgRP}$ mice. Taken together, these results reveal a critical role of hypothalamic AgRP neuron-derived c-Jun in orchestrating chronic stress-induced anxiety-like behaviors and colitis susceptibility. These results provide a new perspective for understanding the neuronal mechanisms and potential therapeutic target for the comorbidity of psychiatric disorders, such as anxiety, and IBD.

Keywords: AgRP neurons; Anxiety; Brain-gut axis; c-Jun; Inflammatory bowel

46 disease.

47

48

Introduction

Psychological disorders, such as anxiety and depression, severely influence human health (Kalin, 2020). What makes it even worse is that they are frequently associated with the occurrence of many other diseases, including inflammatory bowel diseases (IBD) (Kurina et al., 2001; Wang et al., 2020; Xia et al., 2021). Stress is a common cause of psychiatric disorders (de Kloet et al., 2005) and intestinal inflammation (Gao et al., 2018; Qiu et al., 1999). Accumulating lines of evidence has illustrated that brain-gut interactions play an important role in the outcome of psychological disorders and IBD under stress conditions (Bonaz and Bernstein, 2013; Gracie et al., 2019). Although gut signals and microbiota are proposed to play roles in the comorbidity of psychological disorders and intestinal inflammation (Gao et al., 2018), the neural mechanisms behind stress-induced anxiety and colitis susceptibility are unknown.

The hypothalamus is an important neural control center in the regulation of the stress response (Bains et al., 2015), consisting of a series of important nuclei. The hypothalamic arcuate nucleus (ARC) is critical to the regulation of energy metabolism (Sohn et al., 2013) and recently reported to be engaged in emotional regulation (Fang et al., 2021; Qu et al., 2020; Xia et al., 2021). There are two specific populations of neurons in the ARC: neurons co-expressing the orexigenic neuropeptide agouti-related protein (AgRP) and neuropeptide Y, and neurons co-expressing the anorexigenic pro-opiomelanocortin (POMC) precursor and the cocaine- and amphetamine-related transcript, whereas the AGRP/NPY neurons have an inhibitory

effect on the POMC/CART neurons (Bell et al., 2005). Unlike the POMC that is widely produced in addition to ARC (Harno et al., 2018), neurons expressing AgRP are localized exclusively in the hypothalamic ARC (Broberger et al., 1998). AgRP neuronal activity is influenced by stress (Fang et al., 2021), and controls diverse physiological processes, including feeding (Bell et al., 2005), pain sensation (Alhadeff et al., 2018) and food-seeking behavior (Dietrich et al., 2015). Studies shows that AgRP neurons are involved in the regulation of peripheral tissue homeostasis (Joly-Amado et al., 2012; Kim et al., 2015), suggesting that it may play an important role in stress-induced anxiety and colitis.

c-Jun is a component of the activator protein-1 transcription factor family, which forms either a homodimer or heterodimer with other members of the family (c-Fos or ATF) and plays a role in the activation of downstream target genes (Wisdom et al., 1999). It is expressed in many tissues, including brain (Sakai et al., 1989). c-Jun is shown to be involved in the regulation of many functions in peripheral tissues (Fuest et al., 2012; Nateri et al., 2005). By contrast, the role of c-Jun in the brain is poorly understood, except for some biological processes such as axonal injury (Raivich et al., 2004) and neurodegeneration (Raivich and Behrens, 2006). Because c-Jun is an immediate-early gene that is dynamically regulated in response to neuronal activity (McNeill and Robinson, 2015), it is commonly used as a marker reflecting neuronal activity (Hoffman et al., 1993). However, it is also induced under stress conditions (Filipovic et al., 2012) and highly expressed in the hypothalamus arcuate nucleus (Herdegen et al., 1995), suggesting that it may additionally be involved in the

regulation of some important functions in the arcuate nucleus.

Based on the above knowledge, we hypothesize that c-Jun in AgRP neurons plays an important role in the stress-induced comorbidity of anxiety and IBD. This study investigates such a possibility and explores the likely mechanisms.

Results

Chronic Restraint Stress (CRS) Induces Anxiety-Like Behaviors and Increases Susceptibility to Colitis

To induce anxiety and colitis, we employed a CRS mouse model (Supplementary information Fig. S1A) as described previously (Gao et al., 2018; Liu et al., 2020; McGill et al., 2006), which significantly reduced body weight, elevated adrenal gland weight and serum corticosterone levels compared with control treatment (Supplementary information Fig. S1B-D). As shown previously (Liu et al., 2020), CRS induced anxiety-like behaviors, as demonstrated by the significantly reduced time and travel distance in the central region in the open field (OF) test, and the shorter time and fewer entries to the open arms in the elevated plus maze (EPM) test (Supplementary information Fig. S1E and F). In addition, the CRS mice exhibited a greater extent of dextran sodium sulfate (DSS)-induced colitis, as evaluated by the loss of body weight, gross bleeding, and shortening of colon length, as well as histological analysis revealing epithelial damage and lymphocyte infiltration of the distal colon (Supplementary information Fig. S1G-J). Consistently, the mRNA levels

of proinflammatory cytokines (*interleukin (IL)* 6 (*Il6), Il1b, Il12,* and *transforming growth factor beta* (*Tgfb)* (Tian et al., 2019) were significantly increased in the colon tissues of CRS mice (Supplementary information Fig. S1K). These results suggest that CRS could induce anxiety-related behaviors and colitis.

Activation of AgRP Neurons Reverses CRS-increased Anxiety-like behaviors and Colitis Susceptibility

To investigate the involvement of AgRP neurons in CRS-induced effects, we conducted immunofluorescence (IF) staining for c-Fos, a signal reflecting neuronal activity (Krashes et al., 2011), in the AgRP-Cre-Ai9 mice. IF staining of tdTomato (reflecting AgRP neurons) and c-Fos revealed decreased c-Fos levels in the AgRP neurons of CRS mice (Supplementary information Fig. S2A), suggesting inhibited AgRP neuronal activity. If the inhibited AgRP neurons were important in this case, stimulating AgRP neurons by an excitatory DREADD receptor hM3Dq (Krashes et al., 2013), should reverse the CRS-increased susceptibility to anxiety and colitis. As predicted, stimulation of AgRP neurons (as shown by the increased c-Fos staining, Supplementary information Fig. S2B and C) reversed CRS-induced anxiety-like behaviors with an increase in both center time duration and center distance in the OF test (Fig. 1A), and an increase in time and entries into the open arms in the EPM test (Fig. 1B). Furthermore, the activation of AgRP neurons also reversed chronic stress-increased susceptibility to DSS-induced colitis, as demonstrated by its blocking effects on the CRS-induced loss of body weight, increased bleeding score, shortened

colon length, higher histological scores, and increased expression of proinflammatory factors (*Il6, Il1b, Il12,* and *Tgfb)* (Fig. 1C-G, Supplementary information Fig. S2D). Although activation of AgRP neuron has a significant impact on feeding behavior (Krashes et al., 2011), the effect of colitis-related findings was not due to food intake as shown by pair-fed experiments (Supplementary information Fig. S3A-E). These results suggest that activation of AgRP neurons enables to reverse anxiety-related behaviors and colitis induced by CRS.

Inhibition of AgRP Neurons Promotes Anxiety-Like Behaviors and Colitis

To further confirm the role of AgRP neurons in anxiety and colitis, we investigated the phenotypes in mice with inhibition of AgRP neurons, using an inhibitory hM4Di designer receptor exclusively activated by designer drugs (DREADDs) (Krashes et al., 2011), as reflected by the reduced c-Fos immunoreactivity in AgRP neurons (Supplementary information Fig. S4A and B). Interestingly, inhibition of AgRP neurons decreased the center distance and center time in the OF test, and the number of entries and time spent in the open arms in the EPM test, indicating increased anxiety-like behaviors (Fig. 2A and B). Moreover, mice with inhibited neuronal activity of the AgRP were more sensitive to DSS-induced colitis, characterized by a more severe weight loss, gross bleeding, shortened colon length, higher histological scores, and increased pro-inflammatory cytokine levels (*Il6, Il1b, Il12,* and *Tgfb)*, compared with control mice (Fig. 2C–G, Supplementary information Fig. S4C). Collectively, these results indicate that

159 inhibition of AgRP neurons mimics stress-induced anxiety-like behaviors and colitis.

160

161 **Overexpression of c-Jun in AgRP Neurons Confers Resistance to CRS-Induced**

162 **Anxiety-Like Behaviors and Colitis Susceptibility**

163 We then explored the possible involvement of c-Jun in the CRS-induced effects

164 and found that the activity of AgRP neurons decreased through c-Jun ablation and

165 increased through c-Jun overexpression both *in vivo* and *in vitro* (Supplementary

166 information Fig. S5A-D). IF staining confirmed a decrease in c-Jun protein levels in

167 the AgRP neurons of stressed mice (Supplementary information Fig. S6A). If the

168 reduced c-Jun expression was important under stress, the activation of c-Jun in AgRP

169 neurons should be expected to ameliorate CRS-induced effects. To test this possibility,

170 we overexpressed c-Jun in AgRP neurons by injecting AAVs expressing c-Jun into the

171 AgRP-irs-Cre mice (Supplementary information Fig. S6B and C). As predicted, mice

172 with c-Jun overexpression were resistant to CRS-induced weight loss and colon

173 shortening (Supplementary information Fig. S6D and E). Consistently, overexpressed

174 groups spent more time and distance in the center as evaluated in the OF test

175 compared with the control group after CRS (Supplementary information Fig. S6F).

176 Similarly, in the EPM test, groups with overexpressed c-Jun had more entries to the

177 open arm (Supplementary information Fig. S6G). Stressed c-Jun-overexpressing mice

178 were more resistant to DSS-induced body weight loss compared with stressed control

179 mice (Supplementary information Fig. S6H and I). The diarrhea scores and colon

180 length were also relieved in the overexpressed group (Supplementary information Fig.

S6J and K). Furthermore, signs of colon colitis were markedly ameliorated in mice with overexpressed c-Jun, as evidenced by the decreased epithelial damage and lymphocyte infiltration, as well as reduced mRNA expression of inflammatory cytokines (Supplementary information Fig. S6L and M). These data indicate that overexpression of c-Jun in AgRP neurons protected the mice from CRS-induced anxiety and colitis.

Deletion of c-Jun in AgRP Neurons Facilitates Anxiety-Like Behaviors and Colitis

To further confirm the role of c-Jun in AgRP neurons, we generated mice with c-Jun knockdown in AgRP neurons (*c-Jun*$^{\Delta AgRP}$), as confirmed by the reduced c-Jun expression in AgRP neurons (Supplementary information Fig. S7A). The corticosterone concentration was significantly higher in the sera of *c-Jun*$^{\Delta AgRP}$ mice than in control mice, suggesting increased stress (Supplementary information Fig. S7B). Moreover, the body weight of *c-Jun*$^{\Delta AgRP}$ mice was slightly lower than that of control mice (Supplementary information Fig. S7C). Although the classic function of AgRP neurons is to regulate food intake, we did not detect any difference in the change of food intake in *c-Jun*$^{\Delta AgRP}$ mice (Supplementary information Fig. S7D).

The *c-Jun*$^{\Delta AgRP}$ mice displayed obvious anxiety-like behaviors, reflected as a shorter time and less distance in the center in the OF test (Fig. 3A), and fewer entries and time in the open arms as evaluated in the EPM test (Fig. 3B). The clinical signs of colitis, including weight loss, rectal bleeding and colon shortening, were more severe

in *c-Jun*$^{\Delta AgRP}$ mice than in controls after DSS treatment (Fig. 3C-E). The epithelial damage, including mucosal erosion, crypt loss, lymphocyte infiltration, and the mRNA expression of proinflammatory cytokines were also significantly increased in the colons of *c-Jun*$^{\Delta AgRP}$ mice compared with controls (Fig. 3F and G). These data indicate that deletion of *c-Jun* in AgRP neurons is sufficient to induce anxiety-like behaviors and colitis susceptibility in the absence of stress.

Relieving Anxiety with Cyamemazine (CYA) Reverses Colitis in *c-Jun*$^{\Delta AgRP}$ Mice

To investigate whether stimulated anxiety-like behaviors contributed to the increased colitis susceptibility, a typical antipsychotic drug CYA has been shown to block anxiety (Benyamina et al., 2012), was infused into the third ventricle of *c-Jun*$^{\Delta AgRP}$ mice for 7 days. The efficacy of the drug was elevated by the changed 5-HT receptor expression in the ARC (Supplementary information Fig. S8), as CYA is a potent 5-HT receptors antagonist (Benyamina et al., 2012). Interestingly, we found that treatment with CYA largely alleviated anxiety-like behaviors in *c-Jun*$^{\Delta AgRP}$ mice as demonstrated by the OF and EPM tests (Fig. 4A and B). The signs of colitis susceptibility were also alleviated in *c-Jun*$^{\Delta AgRP}$ mice, following evaluation of the examined parameters (Fig. 4C-G). These data indicate that antipsychotic drug may influence the development of colitis in mice with co-existing anxiety.

The Increased Colitis Susceptibility in *c-Jun*$^{\Delta AgRP}$ mice is Mediated by THBS1

Because the brain conveys the neural, endocrine, and circulatory messages to the

gut (Bonaz and Bernstein, 2013; Gracie et al., 2019; Mawdsley and Rampton, 2005), to elucidate the underlying mechanisms of the observed effects, we conducted mass spectrometry to explore the possible secreted proteins in the sera of the mice with c-Jun overexpression and control groups with or without CRS under colitis conditions. We identified 22 secreted proteins that significantly differed in abundance between the three groups (Fig. 5A and B; Supplementary information Table S2-3). Among these proteins, we focused on thrombospondin 1 (THBS1), which showed the most dramatic change and is well known for its anti-angiogenic and anti-inflammatory properties (Adams and Lawler, 2011). The secreted levels of THBS1 were significantly reduced after CRS and notably increased after c-Jun rescue in AgRP neurons (Supplementary information Fig. S9A-C). Moreover, the serum levels of THBS1 were reduced in *c-Jun*$^{\Delta AgRP}$ mice (Fig. 5C) and increased by treatment with CYA (Supplementary information Fig. S9D), indicating it may have potential role in linking anxiety and colitis. To test this hypothesis, we treated *c-Jun*$^{\Delta AgRP}$ mice with THBS1 (Bai et al., 2020) and found that it markedly alleviated colitis, as shown by the resistant effects on the corresponding changes in the body weight loss, bleeding score, colon length, colon histochemical analysis, and the expression of pro-inflammatory factors (Fig. 5D-H). These results suggest that THBS1 suppresses intestinal mucosal inflammation and may serve as a potential biomarker for stress-induced colitis.

Discussion

The brain-gut axis serves as a circuit that incorporates the state of mind and gut signals that ultimately determine the intestinal function (Bonaz and Bernstein, 2013; Gracie et al., 2019; Mawdsley and Rampton, 2005; Wu et al., 2014). Therefore, the changes of brain functions are closely related to gut metabolism abnormalities (Bonaz and Bernstein, 2013; Lee et al., 2021; Mawdsley and Rampton, 2005). Accumulating evidence indicates that mood disorders, such as anxiety or depression, often co-occur with IBD (Blackwell et al., 2021; Gracie et al., 2018; Koloski et al., 2012; Kurina et al., 2001). Several brain areas, including the hypothalamus, hippocampus and amygdala, are involved in anxiety-related behaviors (Adhikari et al., 2010; Bains et al., 2015; Liu et al., 2020). The AgRP neurons in the hypothalamic ARC particularly have gained much attention since more important functions of this neuron were discovered, such as feeding, pain sensation and depression-related behaviors (Alhadeff et al., 2018; Bell et al., 2005; Fang et al., 2021). However, a role of AgRP neurons in the comorbidity of anxiety and colitis has not been reported.

In current study, we used CRS model and chemogenic strategy to investigate the possible involvement of AgRP neurons in stress-induced anxiety and colitis. We found that AgRP neuronal activity was inhibited by CRS. However, in another study under stressed model, AgRP neurons were not affected (Qu et al., 2020). The different response may be attributable to the variation in the duration of treating the mice (4 hours per day in our work versus 1 hour per day in their study), which is likely to result in different levels of stress. The significance of the inhibited AgRP neurons in

CRS was further confirmed by gain- and loss-of AgRP neuron function experiments. To our knowledge, this is the first to demonstrate that convergent regulation of colitis and stress is integrated in the AgRP neurons in the ARC, providing important evidence that psychiatric disorders, such as anxiety, may influence colitis through central neuronal activity in the ARC. Moreover, though some mechanisms are proposed for IBD (Molodecky et al., 2012), the neuronal signals are largely unknown. Our results provide new perspective for understanding the neuronal regulation for IBD. In addition, another study shows that inhibition of AgRP neuron causes depression (Fang et al., 2021), another type of psychiatric disorder (de Kloet et al., 2005), suggesting that AgRP neurons might also play an important role in other psychiatric disorders, as well as diseases related to them. As a number of studies have shown that AgRP neurons facilitate food-seeking behavior (Aponte et al., 2011; Krashes et al., 2011), it remains to be tested whether the role of Agrp neurons in anxiety-like behaviors is influenced by the behaviors driven by feeding. However, the increased food intake did not contribute to the improvement of colitis as evaluated by pair-fed experiments in current study.

We then explored the specific neural molecules regulating stress-induced anxiety and colitis. We found that the expression of the stress-related gene c-Jun was decreased in AgRP neurons under CRS conditions and that knockdown of c-Jun in AgRP neurons mimicked the effect of CRS but reversed these after overexpression of c-Jun. These results demonstrate a novel regulatory role of the central c-Jun in stress-induced anxiety and colitis and provide a potential therapeutic approach for the

treatment of these diseases. However, it is unclear how c-Jun inhibited neuronal activity under stress. Considering that c-Jun plays a role in the regulation of neuron injury and in the promotion of axon regeneration (Raivich et al., 2004), we speculated that stress may lead to the damage of AgRP neurons, thus leading to a change in neuronal activity. However, this possibility requires further investigation.

Moreover, we provided important evidence that anxiety may influence colitis susceptibility by using anxiolytic drug, as well as the possibility for the treatment of IBD with co-existing anxiety. To gain further insights into how anxiety influences colitis, we performed proteomic analysis and serum measurement and found that the levels of secreted protein THBS1 were decreased by CRS in a c-Jun dependent manner, suggesting that it may function as downstream in linking c-Jun regulated anxiety and colitis. Thrombospondins are a family of extracellular matrix proteins, which were first identified in platelets stimulated with thrombin (Baenziger et al., 1971). After treatment with DSS, THBS1-deficient mice show a higher level of crypt damage and deeper lesions, which are reversed by treatment with a THBS1 mimetic peptide (Punekar et al., 2008). The importance of THBS1 in mediating anxiety-associated colitis was confirmed by the reversal effect of recombinant THBS1 on colitis in *c-Jun*$^{\Delta AgRP}$ mice. Because THBS1 levels were correspondingly changed with the status of anxiety and colitis, suggesting that it might be used as a biomarker for the comorbidity of these diseases. However, it remains unclear for the source of secreted THSB1 protein in the sera, as THBS1 can be produced and secreted into the extracellular space of many cell types, including the activated endothelium, intestinal

313 epithelial cells, and astrocytes (Adams and Lawler, 2011; Christopherson et al., 2005;
314 Fang et al., 2015). In addition, the sympathetic nerve and the vagus nerve, which have
315 been shown to be important mediators of central nervous system outputs to the
316 peripheral tissues (Bonaz and Bernstein, 2013; Ghia et al., 2008), may also be
317 involved in the regulation of anxiety-promoted colitis susceptibility. These questions
318 remain for future investigation.

319 Interestingly, we found that chemogenic manipulation or c-Jun knockdown-
320 induced inhibition of AgRP neurons promotes anxiety-like behaviors and colitis in the
321 absence of stressor, suggesting that signals inhibited AgRP neurons may be potential
322 target for the treatment of anxiety and/or colitis. Therefore, our results are also
323 important for understanding the mechanisms for those without obvious stress but
324 present with the comorbidity of psychiatric disorders and IBD.

325 In summary, our present findings revealed that AgRP neuronal activity in the
326 ARC is an important link between anxiety-like behavior and intestinal inflammation
327 (Fig. 5I). The importance of these findings is that we have uncovered the specific
328 neurons and signals in the brain underlying the regulation of the anxiety and colitis
329 comorbidity. Our results provide evidence that CRS-induced anxiety and colitis is
330 mediated through an unexpected neurons AgRP neurons. Moreover, we demonstrated
331 c-Jun as a target in AgRP neuron for stress-induced anxiety and colitis. Furthermore,
332 we identified the secreted protein Thbs1 function in linking anxiety and colitis and as
333 a biomarker for anxiety-colitis comorbidity. These results provide a new perspective
334 for exploring the brain in the regulation of intestinal inflammation homeostasis, and

335 further provide a new central target for the therapeutic intervention of stress-induced
336 psychiatric disorders and intestinal metabolism dysfunction.
337
338
339 # Materials and Methods
340 ## Mice and Treatment
341 Adult male C57BL/6 wild-type (WT) mice were purchased from Shanghai
342 Laboratory Animal Co., Ltd. (Shanghai, China). *c-Jun*$^{loxp/loxp}$ mice (generously
343 provided by Dr. Erwin F. Wagner, Cancer Cell Biology Program, Spanish National
344 Cancer Research Center) were crossed with mice expressing Cre recombinase under
345 control of the AgRP promoter to generate *c-Jun*$^{\Delta AgRP}$ mice. The efficiency of AgRP-
346 specific *c-Jun* deletion was evaluated by mating Ai9 (tdTomato) reporter mice
347 (Madisen et al., 2010) with transgenic mice expressing Cre under control of the AgRP
348 promoter (AgRP-irs-Cre mice), both obtained from Jackson Laboratory (Bar Harbor,
349 ME, USA). Transgenic mice and their littermates were used in experiments at the
350 indicated ages. Mice were subcutaneously injected with recombinant human
351 thrombospondin 1 (THBS1) protein (0.5 mg/kg per day; Novoprotein Scientific Inc.,
352 Shanghai, China) (Bai et al., 2020) or vehicle (phosphate-buffered saline) for the
353 indicated period. To study the effect of anxiolytic drug on anxiety and colitis,
354 cyamemazine (0.25 ug/side, MCE) (Xia et al., 2021) were i.c.v. administrated.
355 Mice were maintained under controlled temperature (23°C), humidity (50–60%),
356 and illumination (12-h light/12-h dark cycle), and provided *ad libitum* access to food

and water. All animal experiments were conducted in accordance with the guidelines of the Institutional Animal Care and Use Committee of Shanghai Institute for Nutritional Sciences, Chinese Academy of Sciences.

Chronic Restraint Stress (CRS) Model

The CRS mouse model was performed as described previously (Gao et al., 2018; Liu et al., 2020). In brief, the mice were individually placed in a 50-mL polypropylene conical tube with multiple holes for ventilation and were restrained to prevent back-and-forth movement. Restraint was applied for 4 h per day from 10:00 a.m. to 2:00 p.m. for the number of days indicated.

Colitis Model Establishment

To establish the dextran sulfate sodium (DSS)-induced colitis model, the drinking water of the mice was supplemented with 3% (w/v) DSS (40 kDa; Aladdin, Shanghai, China) as described previously (Tian et al., 2019), and the colon length was determined at the end of the experiments. Diarrhea scores were assessed as described previously (Rachmilewitz et al., 2002).

Stereotaxic Surgery and Viral Injections

Surgery was performed as reported previously (Yuan et al., 2020) with a stereotaxic frame (Stoelting, Wood Dale, IL, USA). Viral injection coordinates (in mm, midline, bregma, dorsal surface) are as follows: for ARC (± 0.3, 1.5, 5.9), for the third

379 ventricle (0, 1.5, 5.6) (Deng et al., 2017; Xia et al., 2021). To rescue the expression of
380 *c-Jun* specifically localized in AgRP neurons, AgRP-irs-Cre mice were bilaterally
381 injected with 300 nL of a Cre-dependent adeno-associated virus (AAV) vector
382 containing *c-Jun* in the opposite orientation flanked by two inverted loxP sites
383 [AAV9-EF1a-DIO-c-Jun-mCherry, 2.5×10^{12} particle-forming units (PFU)/mL] into
384 the ARC, or with an AAV vector containing only mCherry in the opposite orientation
385 flanked by two inverted loxP sites (AAV9-EF1a-DIO-mCherry, 2.5×10^{12} PFU/mL)
386 as controls.
387
388 **Designer Receptor Exclusively Activated by Designer Drugs (DREADDs)**
389 To inhibit AgRP neuronal activity, AgRP-irs-Cre mice were stereotaxically
390 injected with 300 nL of a Cre-dependent AAV encoding an inhibitory DREADD
391 GPCR (hM4Di) (AAV9-EF1a-DIO-hM4Di-mCherry, 8×10^{12} PFU/mL) or an AAV
392 encoding only mCherry (AAV9-EF1a-DIO-mCherry, 7×10^{12} Pfu/mL) as controls,
393 bilaterally into the ARC.
394 For chemogenetic activation of AgRP neurons, AgRP-irs-Cre mice were
395 stereotaxically injected with 300 nL of a Cre-dependent AAV encoding an excitatory
396 DREADD GPCR (hM3Dq) (AAV9-EF1a-DIO-hM3D(Gq)-mCherry, 3×10^{12}
397 PFU/mL) or an AAV encoding only mCherry (AAV9-EF1a-DIO-mCherry, 3×10^{12}
398 PFU/mL) as controls, bilaterally into the ARC. After 3 weeks of recovery, all mice
399 were then intraperitoneally injected with clozapine N-oxide (CNO)
400 (MedChemExpress, NJ, USA) at 0.3 mg/kg of body weight for hM4Di (Krashes et al.,

2011) silencing and for hM3Dq activation (Krashes *et al.*, 2013) every 12 h for indicated days.

Isolation and Treatment of Primary Hypothalamic Neurons

The mouse primary cultures of hypothalamic neurons were referred as previously described (Deng et al., 2018). sh-c-Jun and c-Jun over-expressed (pCMV-c-Jun) plasmid were transfected into cells using lipofectamine 3000 reagent (Invitrogen; Carlsbad, CA, USA) according to the manufacturer's recommendation. The shRNA sequence for mouse c-Jun was 5'-GCTAACGCAGCAGTTGCAAAC-3'.

Open Field (OF) Test

The OF test was performed as in previous studies (Fan et al., 2019; Liu et al., 2020). In brief, a white open field box (50 × 50 × 50 cm; length × width × height) was divided into a center field (25 × 25 cm) and a periphery field for analysis purposes. The track was analyzed using LabState (AniLab) by recognizing the central body point of the mouse throughout a 10-min session. Less time and locomotion spent in the center of the box were interpreted as anxiety-like behaviors.

Elevated Plus Maze (EPM) Test

The EPM test was performed as previously described (Fan et al., 2019; Liu et al., 2020). The elevated plus maze made of plastic and consisted of two white open arms without walls and two white enclosed arms with walls (25-cm long, 5-cm wide, 15-

cm high). The maze was placed 60 cm above the floor. Mice were introduced into the center quadrant with their back facing an open arm. The ANY-maze video tracking system (Anilab) was used to track and analyze the time of mice spent in the open arms and their entries into the open arms throughout a 10-min session. Anxiety was evaluated by fewer movements into the open arms and less time spent there.

RNA Isolation and Quantitative Real-time (qRT)-PCR

RNA extraction and qRT-PCR were performed as described previously (Deng et al., 2018). The primer sequences used in this study are provided in Supplementary information, Table S1

Histological Scoring

Histological scoring was performed as described previously (Hu et al., 2019). Hematoxylin and eosin (H&E)-staining of colonic tissue sections were scored in a blinded fashion for determining the degree of inflammation and tissue damage on separate scales from 0 to 6.

Serum Measurements

The proteomics was performed by the serum after removing common high-abundance protein through using a Thermo Fisher's serum High Abundance protein removal reag ent (High Select™ Top14 Abundant Protein Depletion Mini Spin Columns, A36370, Thermo fisher, US). The mass spectrometer Thermo Scientific Q Exactive was perfor

med for Label-free quantification detection and data was analyzed by Proteome Discoverer 2.2. The secreted proteins with fold change (FC) $\geqslant$1.5 and p-value < 0.05 were considered to be differential proteins. Volcano plots were used to filter the proteins of interest which based on $\log_2$(FC) and -$\log_{10}$(P-value) of the secreted proteins (Zhu et al., 2011). The raw data is available in the link: https://datadryad.org/stash/share/20xmGKT2z--QNG0ebHfHU8FR8Vy96LuKXe4AhPwHWc4. Serum corticosterone levels were measured with an enzyme-linked immunosorbent assay (ELISA) kit (ADI-901-097; Enzo Life Science, Farmingdale, NY, USA) as described previously (Lee et al., 2020). The THBS1 levels were measured using an ELISA kit (mlbio, Shanghai, China) according to the manufacturer's recommendations.

Immunofluorescence (IF) Staining

Immunofluorescence staining was performed as described previously (Yuan et al., 2020) with primary antibodies to c-Jun (1:1000, Cell Signaling Technology, Danvers, MA, USA) and c-Fos (1:1000, Cell Signaling Technology, mAb2250 or 1:500, Santa Cruz Biotechnology, Santa Cruz, CA, USA). c-Fos staining was coupled with a TSA Plus Fluorescein KIT (NEL741001KT, Perkinelmer, Waltham, MA, USA).

Statistical Analysis

Experimental data are expressed as the mean ± standard error of the mean (SEM) of the number of tests stated for each experiment. Statistical comparisons were made using either two-tailed Student's *t* test or two-way analysis of variance, followed by

Tukey's multiple comparisons test, as indicated in the figure legends. All statistical tests were performed using GraphPad Prism, version 8.0 (GraphPad Software, San Diego, CA, USA). In addition, the individual data points on each graph were shown in order to reflect the individual variability of the measures. *P <0.05, **P <0.01.

Acknowledgements

We would like to thank Dr. Erwin F. Wagner (Cancer Cell Biology Program, Spanish National Cancer Research Center) and Lijian Hui (Chinese Academy of Sciences Center for Excellence in Molecular Cell Science) for providing c-Jun loxp/loxp mice.

Author Contributions

Fuxin Jiao, Zhanju Liu and Feifan Guo designed the project and analyzed the data; Fuxin Jiao, Xiaoming Hu, Hanrui Yin, Feixiang Yuan, Ziheng Zhou performed the experiments; Fuxin Jiao, Zhanju Liu, and Feifan Guo wrote the manuscript. Wei Wu and Shanghai Chen provided experimental materials; All authors discussed and revised the manuscript.

Conflict of interest

The authors disclose no conflicts.

Funding

This work is supported by grant from The National Key R&D Program of China (2018YFA0800600), the National Natural Science Foundation (91957207, 31830044, 81870592, 82170868, 81770852, 81970742, 81970731, 82000764 and 91942312), and Shanghai leading talent program, CAS Interdisciplinary Innovation Team, Novo Nordisk-Chinese Academy of Sciences Research Fund (NNCAS-2008-10). Natural Science Foundation of Shanghai "science and technology innovation action plan" (21ZR1475900).

References

Adams, J.C., and Lawler, J. (2011). The thrombospondins. Cold Spring Harb Perspect Biol *3*, a009712. 10.1101/cshperspect.a009712.

Adhikari, A., Topiwala, M.A., and Gordon, J.A. (2010). Synchronized activity between the ventral hippocampus and the medial prefrontal cortex during anxiety. Neuron *65*, 257-269. 10.1016/j.neuron.2009.12.002.

Alhadeff, A.L., Su, Z., Hernandez, E., Klima, M.L., Phillips, S.Z., Holland, R.A., Guo, C., Hantman, A.W., De Jonghe, B.C., and Betley, J.N. (2018). A Neural Circuit for the Suppression of Pain by a Competing Need State. Cell *173*, 140-152 e115. 10.1016/j.cell.2018.02.057.

Aponte, Y., Atasoy, D., and Sternson, S.M. (2011). AGRP neurons are sufficient to orchestrate feeding behavior rapidly and without training. Nat Neurosci *14*, 351-355. 10.1038/nn.2739.

Baenziger, N.L., Brodie, G.N., and Majerus, P.W. (1971). A thrombin-sensitive protein of human platelet membranes. Proc Natl Acad Sci U S A *68*, 240-243. 10.1073/pnas.68.1.240.

Bai, J., Xia, M., Xue, Y., Ma, F., Cui, A., Sun, Y., Han, Y., Xu, X., Zhang, F., Hu, Z., et al. (2020). Thrombospondin 1 improves hepatic steatosis in diet-induced insulin-resistant mice and is associated with hepatic fat content in humans. EBioMedicine *57*, 102849. 10.1016/j.ebiom.2020.102849.

Bains, J.S., Wamsteeker Cusulin, J.I., and Inoue, W. (2015). Stress-related synaptic plasticity in the hypothalamus. Nat Rev Neurosci *16*, 377-388. 10.1038/nrn3881.

Bell, C.G., Walley, A.J., and Froguel, P. (2005). The genetics of human obesity. Nat Rev Genet *6*, 221-234. 10.1038/nrg1556.

Benyamina, A., Naassila, M., and Bourin, M. (2012). Potential role of cortical 5-HT(2A) receptors in the anxiolytic action of cyamemazine in benzodiazepine withdrawal. Psychiatry Res *198*, 307-312. 10.1016/j.psychres.2012.01.009.

Blackwell, J., Saxena, S., Petersen, I., Hotopf, M., Creese, H., Bottle, A., Alexakis, C., Pollok, R.C., and group, P.-I.s. (2021). Depression in individuals who subsequently develop inflammatory bowel disease:

523 a population-based nested case-control study. Gut *70*, 1642-1648. 10.1136/gutjnl-2020-322308.
524 Bonaz, B.L., and Bernstein, C.N. (2013). Brain-gut interactions in inflammatory bowel disease.
525 Gastroenterology *144*, 36-49. 10.1053/j.gastro.2012.10.003.
526 Broberger, C., Johansen, J., Johansson, C., Schalling, M., and Hokfelt, T. (1998). The neuropeptide
527 Y/agouti gene-related protein (AGRP) brain circuitry in normal, anorectic, and monosodium glutamate-
528 treated mice. Proc Natl Acad Sci U S A *95*, 15043-15048. 10.1073/pnas.95.25.15043.
529 Christopherson, K.S., Ullian, E.M., Stokes, C.C., Mullowney, C.E., Hell, J.W., Agah, A., Lawler, J., Mosher,
530 D.F., Bornstein, P., and Barres, B.A. (2005). Thrombospondins are astrocyte-secreted proteins that
531 promote CNS synaptogenesis. Cell *120*, 421-433. 10.1016/j.cell.2004.12.020.
532 de Kloet, E.R., Joels, M., and Holsboer, F. (2005). Stress and the brain: from adaptation to disease. Nat
533 Rev Neurosci *6*, 463-475. 10.1038/nrn1683.
534 Deng, J., Yuan, F., Guo, Y., Xiao, Y., Niu, Y., Deng, Y., Han, X., Guan, Y., Chen, S., and Guo, F. (2017).
535 Deletion of ATF4 in AgRP Neurons Promotes Fat Loss Mainly via Increasing Energy Expenditure.
536 Diabetes *66*, 640-650. 10.2337/db16-0954.
537 Deng, Y., Xiao, Y., Yuan, F., Liu, Y., Jiang, X., Deng, J., Fejes-Toth, G., Naray-Fejes-Toth, A., Chen, S., Chen,
538 Y., et al. (2018). SGK1/FOXO3 Signaling in Hypothalamic POMC Neurons Mediates Glucocorticoid-
539 Increased Adiposity. Diabetes *67*, 569-580. 10.2337/db17-1069.
540 Dietrich, M.O., Zimmer, M.R., Bober, J., and Horvath, T.L. (2015). Hypothalamic Agrp neurons drive
541 stereotypic behaviors beyond feeding. Cell *160*, 1222-1232. 10.1016/j.cell.2015.02.024.
542 Fan, K.Q., Li, Y.Y., Wang, H.L., Mao, X.T., Guo, J.X., Wang, F., Huang, L.J., Li, Y.N., Ma, X.Y., Gao, Z.J., et al.
543 (2019). Stress-Induced Metabolic Disorder in Peripheral CD4(+) T Cells Leads to Anxiety-like Behavior.
544 Cell *179*, 864-879 e819. 10.1016/j.cell.2019.10.001.
545 Fang, L.L., Yu, H.Q., Wu, R.J., He, C., Li, M., Yan, H., Li, J.J., Wang, S., Liu, Z.G., Liu, Z.J., and Yang, P.C.
546 (2015). Thrombospondin 1 Modulates Monocyte Properties to Suppress Intestinal Mucosal
547 Inflammation. J Innate Immun *7*, 601-611. 10.1159/000398799.
548 Fang, X., Jiang, S., Wang, J., Bai, Y., Kim, C.S., Blake, D., Weintraub, N.L., Lei, Y., and Lu, X.Y. (2021).
549 Chronic unpredictable stress induces depression-related behaviors by suppressing AgRP neuron
550 activity. Molecular psychiatry. 10.1038/s41380-020-01004-x.
551 Filipovic, D., Zlatkovic, J., Pavicevic, I., Mandic, L., and Demajo, M. (2012). Chronic isolation stress
552 compromises JNK/c-Jun signaling in rat brain. J Neural Transm (Vienna) *119*, 1275-1284.
553 10.1007/s00702-012-0776-0.
554 Fuest, M., Willim, K., MacNelly, S., Fellner, N., Resch, G.P., Blum, H.E., and Hasselblatt, P. (2012). The
555 transcription factor c-Jun protects against sustained hepatic endoplasmic reticulum stress thereby
556 promoting hepatocyte survival. Hepatology *55*, 408-418. 10.1002/hep.24699.
557 Gao, X., Cao, Q., Cheng, Y., Zhao, D., Wang, Z., Yang, H., Wu, Q., You, L., Wang, Y., Lin, Y., et al. (2018).
558 Chronic stress promotes colitis by disturbing the gut microbiota and triggering immune system
559 response. Proc Natl Acad Sci U S A *115*, E2960-E2969. 10.1073/pnas.1720696115.
560 Ghia, J.E., Blennerhassett, P., and Collins, S.M. (2008). Impaired parasympathetic function increases
561 susceptibility to inflammatory bowel disease in a mouse model of depression. The Journal of clinical
562 investigation *118*, 2209-2218. 10.1172/JCI32849.
563 Gracie, D.J., Guthrie, E.A., Hamlin, P.J., and Ford, A.C. (2018). Bi-directionality of Brain-Gut Interactions
564 in Patients With Inflammatory Bowel Disease. Gastroenterology *154*, 1635-1646 e1633.
565 10.1053/j.gastro.2018.01.027.
566 Gracie, D.J., Hamlin, P.J., and Ford, A.C. (2019). The influence of the brain-gut axis in inflammatory

bowel disease and possible implications for treatment. Lancet Gastroenterol Hepatol *4*, 632-642. 10.1016/S2468-1253(19)30089-5.

Harno, E., Gali Ramamoorthy, T., Coll, A.P., and White, A. (2018). POMC: The Physiological Power of Hormone Processing. Physiol Rev *98*, 2381-2430. 10.1152/physrev.00024.2017.

Herdegen, T., Kovary, K., Buhl, A., Bravo, R., Zimmermann, M., and Gass, P. (1995). Basal expression of the inducible transcription factors c-Jun, JunB, JunD, c-Fos, FosB, and Krox-24 in the adult rat brain. J Comp Neurol *354*, 39-56. 10.1002/cne.903540105.

Hoffman, G.E., Smith, M.S., and Verbalis, J.G. (1993). c-Fos and related immediate early gene products as markers of activity in neuroendocrine systems. Front Neuroendocrinol *14*, 173-213. 10.1006/frne.1993.1006.

Hu, X., Deng, J., Yu, T., Chen, S., Ge, Y., Zhou, Z., Guo, Y., Ying, H., Zhai, Q., Chen, Y., et al. (2019). ATF4 Deficiency Promotes Intestinal Inflammation in Mice by Reducing Uptake of Glutamine and Expression of Antimicrobial Peptides. Gastroenterology *156*, 1098-1111. 10.1053/j.gastro.2018.11.033.

Joly-Amado, A., Denis, R.G., Castel, J., Lacombe, A., Cansell, C., Rouch, C., Kassis, N., Dairou, J., Cani, P.D., Ventura-Clapier, R., et al. (2012). Hypothalamic AgRP-neurons control peripheral substrate utilization and nutrient partitioning. The EMBO journal *31*, 4276-4288. 10.1038/emboj.2012.250.

Kalin, N.H. (2020). Novel Insights Into Pathological Anxiety and Anxiety-Related Disorders. Am J Psychiatry *177*, 187-189. 10.1176/appi.ajp.2020.20010057.

Kim, J.G., Sun, B.H., Dietrich, M.O., Koch, M., Yao, G.Q., Diano, S., Insogna, K., and Horvath, T.L. (2015). AgRP Neurons Regulate Bone Mass. Cell reports *13*, 8-14. 10.1016/j.celrep.2015.08.070.

Koloski, N.A., Jones, M., Kalantar, J., Weltman, M., Zaguirre, J., and Talley, N.J. (2012). The brain--gut pathway in functional gastrointestinal disorders is bidirectional: a 12-year prospective population-based study. Gut *61*, 1284-1290. 10.1136/gutjnl-2011-300474.

Krashes, M.J., Koda, S., Ye, C., Rogan, S.C., Adams, A.C., Cusher, D.S., Maratos-Flier, E., Roth, B.L., and Lowell, B.B. (2011). Rapid, reversible activation of AgRP neurons drives feeding behavior in mice. The Journal of clinical investigation *121*, 1424-1428. 10.1172/JCI46229.

Krashes, M.J., Shah, B.P., Koda, S., and Lowell, B.B. (2013). Rapid versus delayed stimulation of feeding by the endogenously released AgRP neuron mediators GABA, NPY, and AgRP. Cell Metab *18*, 588-595. 10.1016/j.cmet.2013.09.009.

Kurina, L.M., Goldacre, M.J., Yeates, D., and Gill, L.E. (2001). Depression and anxiety in people with inflammatory bowel disease. J Epidemiol Community Health *55*, 716-720. 10.1136/jech.55.10.716.

Lee, H.S., Lobbestael, E., Vermeire, S., Sabino, J., and Cleynen, I. (2021). Inflammatory bowel disease and Parkinson's disease: common pathophysiological links. Gut *70*, 408-417. 10.1136/gutjnl-2020-322429.

Lee, J.E., Kwon, H.J., Choi, J., Seo, J.S., and Han, P.L. (2020). Aging increases vulnerability to stress-induced depression via upregulation of NADPH oxidase in mice. Commun Biol *3*, 292. 10.1038/s42003-020-1010-5.

Liu, W.Z., Zhang, W.H., Zheng, Z.H., Zou, J.X., Liu, X.X., Huang, S.H., You, W.J., He, Y., Zhang, J.Y., Wang, X.D., and Pan, B.X. (2020). Identification of a prefrontal cortex-to-amygdala pathway for chronic stress-induced anxiety. Nature communications *11*, 2221. 10.1038/s41467-020-15920-7.

Madisen, L., Zwingman, T.A., Sunkin, S.M., Oh, S.W., Zariwala, H.A., Gu, H., Ng, L.L., Palmiter, R.D., Hawrylycz, M.J., Jones, A.R., et al. (2010). A robust and high-throughput Cre reporting and characterization system for the whole mouse brain. Nat Neurosci *13*, 133-140. 10.1038/nn.2467.

Mawdsley, J.E., and Rampton, D.S. (2005). Psychological stress in IBD: new insights into pathogenic and

611 therapeutic implications. Gut *54*, 1481-1491. 10.1136/gut.2005.064261.
612 McGill, B.E., Bundle, S.F., Yaylaoglu, M.B., Carson, J.P., Thaller, C., and Zoghbi, H.Y. (2006). Enhanced
613 anxiety and stress-induced corticosterone release are associated with increased Crh expression in a
614 mouse model of Rett syndrome. Proc Natl Acad Sci U S A *103*, 18267-18272.
615 10.1073/pnas.0608702103.
616 McNeill, M.S., and Robinson, G.E. (2015). Voxel-based analysis of the immediate early gene, c-jun, in
617 the honey bee brain after a sucrose stimulus. Insect Mol Biol *24*, 377-390. 10.1111/imb.12165.
618 Molodecky, N.A., Soon, I.S., Rabi, D.M., Ghali, W.A., Ferris, M., Chernoff, G., Benchimol, E.I.,
619 Panaccione, R., Ghosh, S., Barkema, H.W., and Kaplan, G.G. (2012). Increasing incidence and
620 prevalence of the inflammatory bowel diseases with time, based on systematic review.
621 Gastroenterology *142*, 46-54 e42; quiz e30. 10.1053/j.gastro.2011.10.001.
622 Nateri, A.S., Spencer-Dene, B., and Behrens, A. (2005). Interaction of phosphorylated c-Jun with TCF4
623 regulates intestinal cancer development. Nature *437*, 281-285. 10.1038/nature03914.
624 Punekar, S., Zak, S., Kalter, V.G., Dobransky, L., Punekar, I., Lawler, J.W., and Gutierrez, L.S. (2008).
625 Thrombospondin 1 and its mimetic peptide ABT-510 decrease angiogenesis and inflammation in a
626 murine model of inflammatory bowel disease. Pathobiology *75*, 9-21. 10.1159/000113790.
627 Qiu, B.S., Vallance, B.A., Blennerhassett, P.A., and Collins, S.M. (1999). The role of CD4+ lymphocytes
628 in the susceptibility of mice to stress-induced reactivation of experimental colitis. Nature medicine *5*,
629 1178-1182. 10.1038/13503.
630 Qu, N., He, Y., Wang, C., Xu, P., Yang, Y., Cai, X., Liu, H., Yu, K., Pei, Z., Hyseni, I., et al. (2020). A POMC-
631 originated circuit regulates stress-induced hypophagia, depression, and anhedonia. Molecular
632 psychiatry *25*, 1006-1021. 10.1038/s41380-019-0506-1.
633 Rachmilewitz, D., Karmeli, F., Takabayashi, K., Hayashi, T., Leider-Trejo, L., Lee, J., Leoni, L.M., and Raz,
634 E. (2002). Immunostimulatory DNA ameliorates experimental and spontaneous murine colitis.
635 Gastroenterology *122*, 1428-1441. 10.1053/gast.2002.32994.
636 Raivich, G., and Behrens, A. (2006). Role of the AP-1 transcription factor c-Jun in developing, adult and
637 injured brain. Prog Neurobiol *78*, 347-363. 10.1016/j.pneurobio.2006.03.006.
638 Raivich, G., Bohatschek, M., Da Costa, C., Iwata, O., Galiano, M., Hristova, M., Nateri, A.S., Makwana,
639 M., Riera-Sans, L., Wolfer, D.P., et al. (2004). The AP-1 transcription factor c-Jun is required for efficient
640 axonal regeneration. Neuron *43*, 57-67. 10.1016/j.neuron.2004.06.005.
641 Sakai, M., Okuda, A., Hatayama, I., Sato, K., Nishi, S., and Muramatsu, M. (1989). Structure and
642 expression of the rat c-jun messenger RNA: tissue distribution and increase during chemical
643 hepatocarcinogenesis. Cancer research *49*, 5633-5637.
644 Sohn, J.W., Elmquist, J.K., and Williams, K.W. (2013). Neuronal circuits that regulate feeding behavior
645 and metabolism. Trends Neurosci *36*, 504-512. 10.1016/j.tins.2013.05.003.
646 Tian, Y., Xu, J., Li, Y., Zhao, R., Du, S., Lv, C., Wu, W., Liu, R., Sheng, X., Song, Y., et al. (2019). MicroRNA-
647 31 Reduces Inflammatory Signaling and Promotes Regeneration in Colon Epithelium, and Delivery of
648 Mimics in Microspheres Reduces Colitis in Mice. Gastroenterology *156*, 2281-2296 e2286.
649 10.1053/j.gastro.2019.02.023.
650 Wang, Y.H., Li, J.Q., Shi, J.F., Que, J.Y., Liu, J.J., Lappin, J.M., Leung, J., Ravindran, A.V., Chen, W.Q., Qiao,
651 Y.L., et al. (2020). Depression and anxiety in relation to cancer incidence and mortality: a systematic
652 review and meta-analysis of cohort studies. Molecular psychiatry *25*, 1487-1499. 10.1038/s41380-019-
653 0595-x.
654 Wisdom, R., Johnson, R.S., and Moore, C. (1999). c-Jun regulates cell cycle progression and apoptosis

by distinct mechanisms. The EMBO journal *18*, 188-197. 10.1093/emboj/18.1.188.

Wu, W., Sun, M., Zhang, H.P., Chen, T., Wu, R., Liu, C., Yang, G., Geng, X.R., Feng, B.S., Liu, Z., et al. (2014). Prolactin mediates psychological stress-induced dysfunction of regulatory T cells to facilitate intestinal inflammation. Gut *63*, 1883-1892. 10.1136/gutjnl-2013-306083.

Xia, G., Han, Y., Meng, F., He, Y., Srisai, D., Farias, M., Dang, M., Palmiter, R.D., Xu, Y., and Wu, Q. (2021). Reciprocal control of obesity and anxiety-depressive disorder via a GABA and serotonin neural circuit. Molecular psychiatry. 10.1038/s41380-021-01053-w.

Yuan, F., Jiang, H., Yin, H., Jiang, X., Jiao, F., Chen, S., Ying, H., Chen, Y., Zhai, Q., and Guo, F. (2020). Activation of GCN2/ATF4 signals in amygdalar PKC-delta neurons promotes WAT browning under leucine deprivation. Nature communications *11*, 2847. 10.1038/s41467-020-16662-2.

Zhu, P., Bowden, P., Zhang, D., and Marshall, J.G. (2011). Mass spectrometry of peptides and proteins from human blood. Mass Spectrom Rev *30*, 685-732. 10.1002/mas.20291.

683

Figure legends

685 **Figure 1.** Activation of AgRP neurons reverses CRS-induced anxiety behaviors and
686 colitis. (A) Representative tracks and statistical results in OF test. (B) Representative
687 tracks and statistics in EPM test. (C) Percentage of body weight loss. (D) Scores of
688 diarrhea. (E) Gross morphology and length of the colon. (F) H&E staining and
689 histological scores of the colon tissues. Scale bar, 110 μm. (G) qRT-PCR analysis of
690 mRNA expression of inflammatory cytokines (*Il6, Il1b, Il12,* and *Tgfb*) in the distal
691 colon tissues. Studies for A-B were conducted using 10- to 12-week-old AgRP-Cre
692 mice receiving AAV expressing mCherry (- hM3Dq) or hM3Dq (+ hM3Dq), all mice
693 experienced unstressed (- CRS) or stressed (+ CRS) treatment for 14 days. Behavioral
694 tests were performed 30 min after single CNO injection on day 15 (A) and day 16 (B).
695 C-G were performed using - hM3Dq mice and + hM3Dq mice under treatment of 3%
696 DSS in drinking water for 7 days to induce acute colitis with (+ CRS) or without (-
697 CRS) stress, simultaneously receiving CNO injections every 12 hours per day. Values
698 are expressed as means ± SEM (n = 5-8 per group), with individual data points. Data
699 were analyzed using two-way analysis of variance, followed by Tukey's multiple
700 comparisons test. - hM3Dq + CRS versus - hM3Dq - CRS, *P <0.05, **P <0.01; +
701 hM3Dq + CRS versus - hM3Dq + CRS, $^{\#}$P <0.05, $^{\#\#}$P <0.01 (C-D).

702

703 **Figure 2.** Inhibition of AgRP neurons mimics CRS-increased susceptibility to anxiety
704 and colitis. (A) Representative tracks and statistical results in OF test. (B)

Representative tracks and statistics in EPM test. (C) Percentage of body weight loss. (D) Scores of diarrhea. (E) Gross morphology and length of the colon. (F) H&E staining and histological scores of the colon tissues. Scale bar, 110 μm. (G) qRT-PCR analysis of mRNA expression of inflammatory cytokines (*Il6, Il1b, Il12,* and *Tgfb*) in the distal colon tissues. Studies for A-B were conducted using 10- to 12-week-old AgRP-Cre mice receiving AAV expressing mCherry (- hM4Di) or hM4Di (+ hM4Di), all mice received CNO injections every 12 h per day. Behavioral tests were performed 30 min after single CNO injection on day 22 (A) and day 23 (B). C-G were performed using - hM4Di mice and + hM4Di mice with 3% DSS in drinking water for 7 days to induce acute colitis after 21 days of CNO injections. Values are expressed as means ± SEM (n = 8-10 per group), with individual data points. Data were analyzed using two-tailed unpaired Student's *t* test.

Figure 3. Deletion of c-Jun in AgRP neurons facilitates anxiety-like behaviors and colitis. (A) Representative tracks and statistical results in OF test. (B) Representative tracks and statistics in EPM test. (C) Percentage of body weight loss. (D) Scores of diarrhea. (E) Gross morphology and length of the colon. (F) H&E staining and histological scores of the colon tissues. Scale bar, 110 μm. (G) qRT-PCR analysis of mRNA expression of inflammatory cytokines (*Il6, Il1b, Il12,* and *Tgfb*) in the distal colonic tissues. Studies for A-B were conducted using 20- to 22-week-old control mice ($c\text{-}Jun^{loxp/loxp}$) or mice with c-Jun deletion in AgRP neurons ($c\text{-}Jun^{\Delta AgRP}$). C-G were performed in $c\text{-}Jun^{loxp/loxp}$ and $c\text{-}Jun^{\Delta AgRP}$ mice administrated with (+ DSS) or

727 without (- DSS) 3% DSS for 6 days to induce acute colitis. Values are expressed as
728 means ± SEM (n = 4-12 per group), with individual data points. Data were analyzed
729 using two-way analysis of variance, followed by Tukey's multiple comparisons test.
730 *c-Jun*$^{loxp/loxp}$ + DSS versus *c-Jun*$^{loxp/loxp}$ - DSS, *P <0.05, **P <0.01. *c-Jun*$^{\Delta AgRP}$ + DSS
731 versus *c-Jun*$^{loxp/loxp}$ + DSS, $^{\#}$P <0.05, $^{\#\#}$P <0.01 (C-D).
732
733 **Figure 4.** Relieving anxiety with cyamemazine (CYA) reverses colitis in *c-Jun*$^{\Delta AgRP}$
734 mice. (A) Representative tracks and statistical results in OF test. (B) Representative
735 tracks and statistics in EPM test. (C) Percentage of body weight loss. (D) Scores of
736 diarrhea. (E) Gross morphology and length of the colon. (F) H&E staining and
737 histological scores of the colon tissues. Scale bar, 110 μm. (G) qRT-PCR analysis of
738 mRNA expression of inflammatory cytokines (*Il6, Il1b, Il12,* and *Tgfb*) in the distal
739 colonic tissues. Studies for A-B were conducted using 18- to 20-week-old *c-Jun*$^{loxp/loxp}$
740 mice and *c-Jun*$^{\Delta AgRP}$ mice treated with (+ CYA) or without (- CYA) CYA for 7 days.
741 Behavioral tests were performed 30 min after single CYA injection on day 8 (A) and
742 day 9 (B). C-G were performed in *c-Jun*$^{loxp/loxp}$ and *c-Jun*$^{\Delta AgRP}$ mice administrated
743 with 3% DSS for 5 days to induce acute colitis with (+ CYA) or without (- CYA) CYA.
744 Values are expressed as means ± SEM (n = 6-10 per group), with individual data
745 points. Data were analyzed using two-way analysis of variance, followed by Tukey's
746 multiple comparisons test. *c-Jun*$^{\Delta AgRP}$ - CYA versus *c-Jun*$^{loxp/loxp}$ - CYA, *P <0.05, **P
747 <0.01. *c-Jun*$^{\Delta AgRP}$ + CYA versus *c-Jun*$^{\Delta AgRP}$- CYA, $^{\#}$P <0.05, $^{\#\#}$P <0.01 (C-D).
748

749 **Figure 5.** The increased colitis susceptibility in *c-Jun*$^{\Delta AgRP}$ mice is mediated by
750 THBS1. (A) Partial least-squares discriminant analysis of protein composition. (B)
751 Spearman's correlation analysis of serum proteome. (C) Serum thbs1 levels. (D)
752 Percentage of body weight loss. (E) Scores of diarrhea. (F) Gross morphology and
753 length of the colon. (G) H&E staining and histological scores of the colon tissues.
754 Scale bar, 110 μm. Scale bar, 110 μm. (H) qRT-PCR analysis of mRNA expression of
755 inflammatory cytokines (*Il6, Il1b, Il12,* and *Tgfb*) in the distal colonic tissues. (I)
756 Summary Diagram. Chronic restraint stress induces anxiety-like behaviors and colitis
757 susceptibility, which is mediated by c-Jun in AgRP neurons. Knockdown of c-Jun in
758 AgRP neurons decreases AgRP neurons activity and increases anxiety-like behaviors
759 and colitis susceptibility through reducing serum THBS1 levels. Studies for A-B were
760 conducted using - c-Jun - CRS mice, - c-Jun + CRS mice and + c-Jun + CRS mice
761 with 3% DSS for 7 days. Serum was collected after DSS stimulation for proteomics
762 profiling. C was conducted using 24- to 26-week-old *c-Jun*$^{loxp/loxp}$ mice and *c-Jun*$^{\Delta AgRP}$
763 mice with DSS administration. D-H were conducted using 22- to 24-week-old *c-*
764 *Jun*$^{loxp/loxp}$ mice and *c-Jun*$^{\Delta AgRP}$ mice with (+ thbs1) or without (- thbs1) thbs1
765 supplementary, simultaneously receiving 3% DSS treatment for 6 days to induce acute
766 colitis. Values are expressed as means ± SEM (n=3-9 per group), with individual data
767 points. Data were analyzed using two-way analysis of variance, followed by Tukey's
768 multiple comparisons test. *c-Jun*$^{\Delta AgRP}$ - thbs1 versus *c-Jun*$^{loxp/loxp}$ - thbs1, *P <0.05,
769 **P <0.01; *c-Jun*$^{\Delta AgRP}$ + thbs1 versus *c-Jun*$^{\Delta AgRP}$ - thbs1, $^{\#}$P <0.05, $^{\#\#}$P <0.01 (D-E).
770

Figure 1

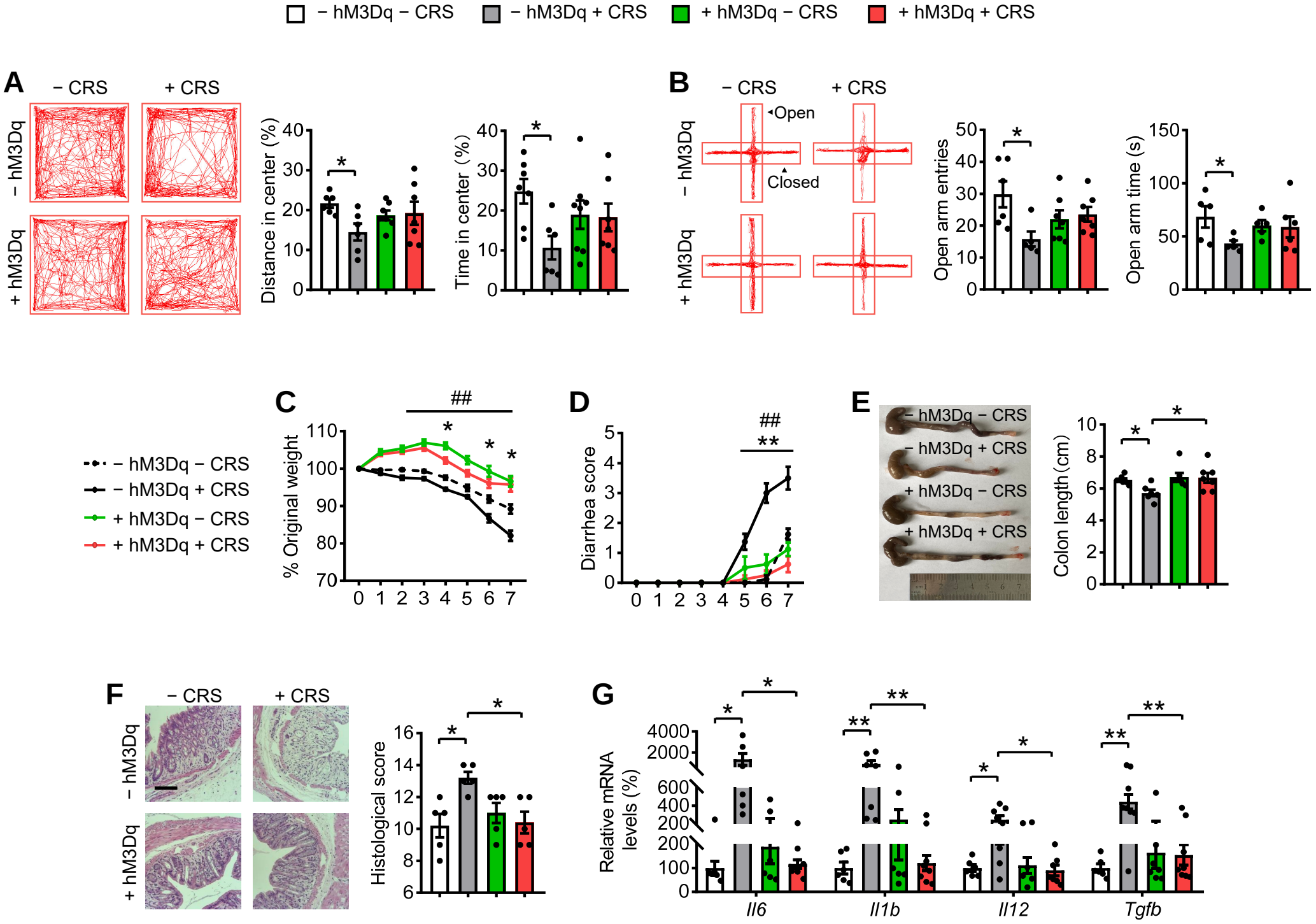
− hM3Dq − CRS
− hM3Dq + CRS
+ hM3Dq − CRS
+ hM3Dq + CRS
A
− CRS
+ CRS
− hM3Dq
+ hM3Dq
Distance in center (%)
Time in center (%)
B
Open
Closed
Open arm entries
Open arm time (s)
C
##
% Original weight
D
Diarrhea score
E
Colon length (cm)
F
Histological score
G
Relative mRNA levels (%)
Il6
Il1b
Il12
Tgfb

Figure 2

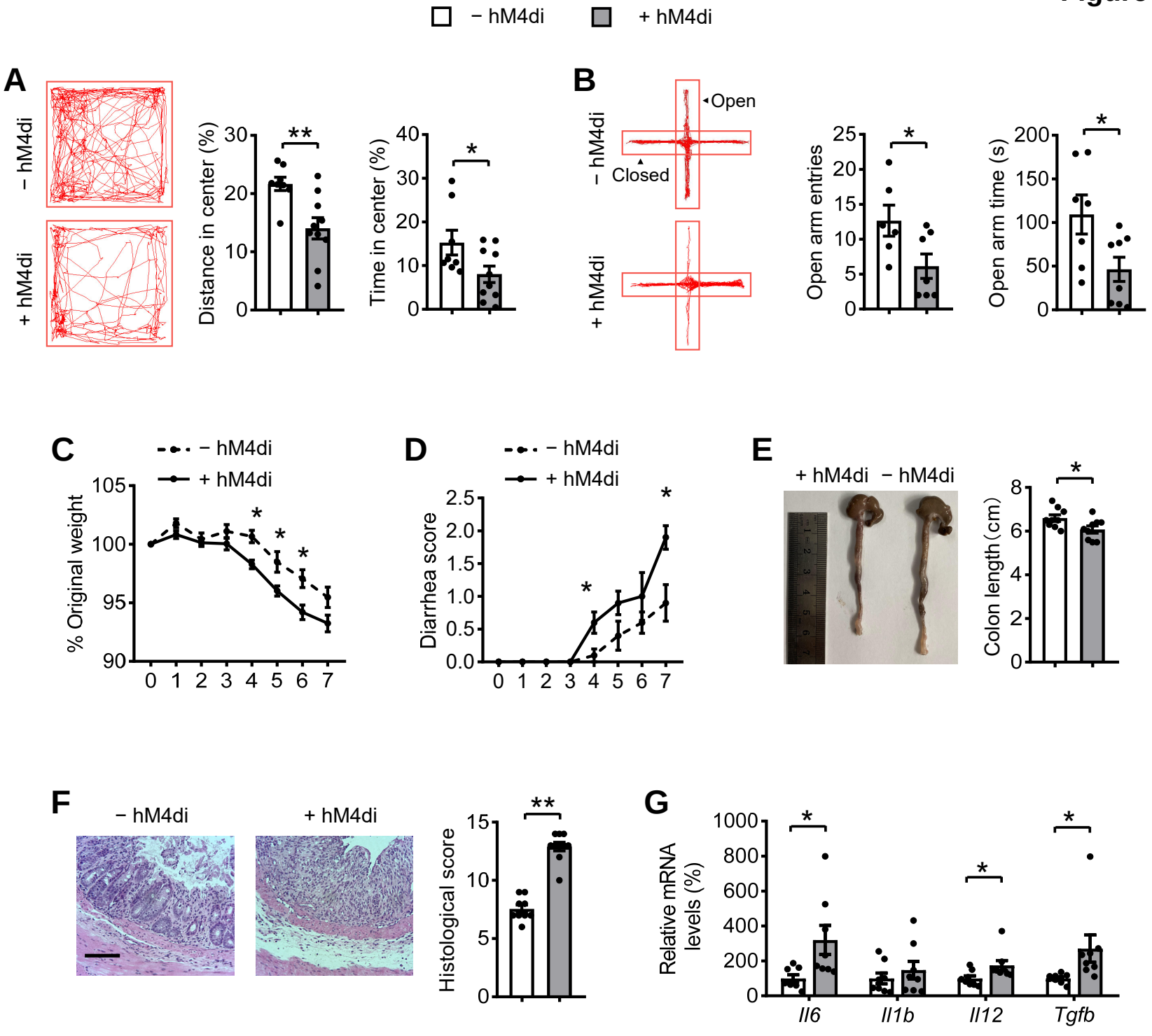
− hM4di
+ hM4di
A
− hM4di
+ hM4di
Distance in center (%)
Time in center (%)
B
Open
Closed
Open arm entries
Open arm time (s)
C
% Original weight
D
Diarrhea score
E
Colon length (cm)
F
Histological score
G
Relative mRNA levels (%)
Il6
Il1b
Il12
Tgfb

Figure 3

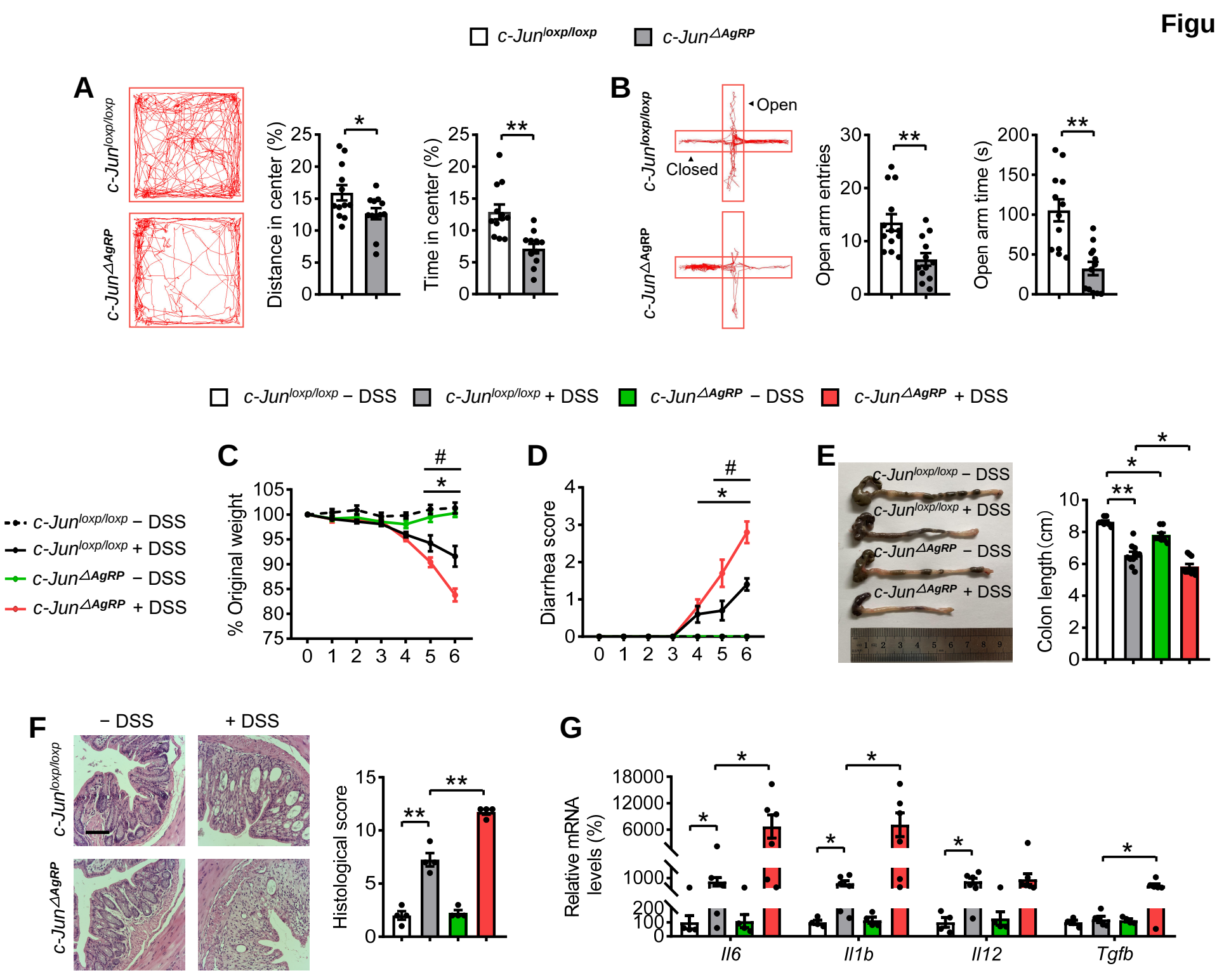
c-Jun loxp/loxp
c-Jun ΔAgRP
A
Distance in center (%)
Time in center (%)
B
Open
Closed
Open arm entries
Open arm time (s)
c-Jun loxp/loxp – DSS
c-Jun loxp/loxp + DSS
c-Jun ΔAgRP – DSS
c-Jun ΔAgRP + DSS
C
% Original weight
D
Diarrhea score
E
Colon length (cm)
F
– DSS
+ DSS
Histological score
G
Relative mRNA levels (%)
Il6
Il1b
Il12
Tgfb

Figure 4

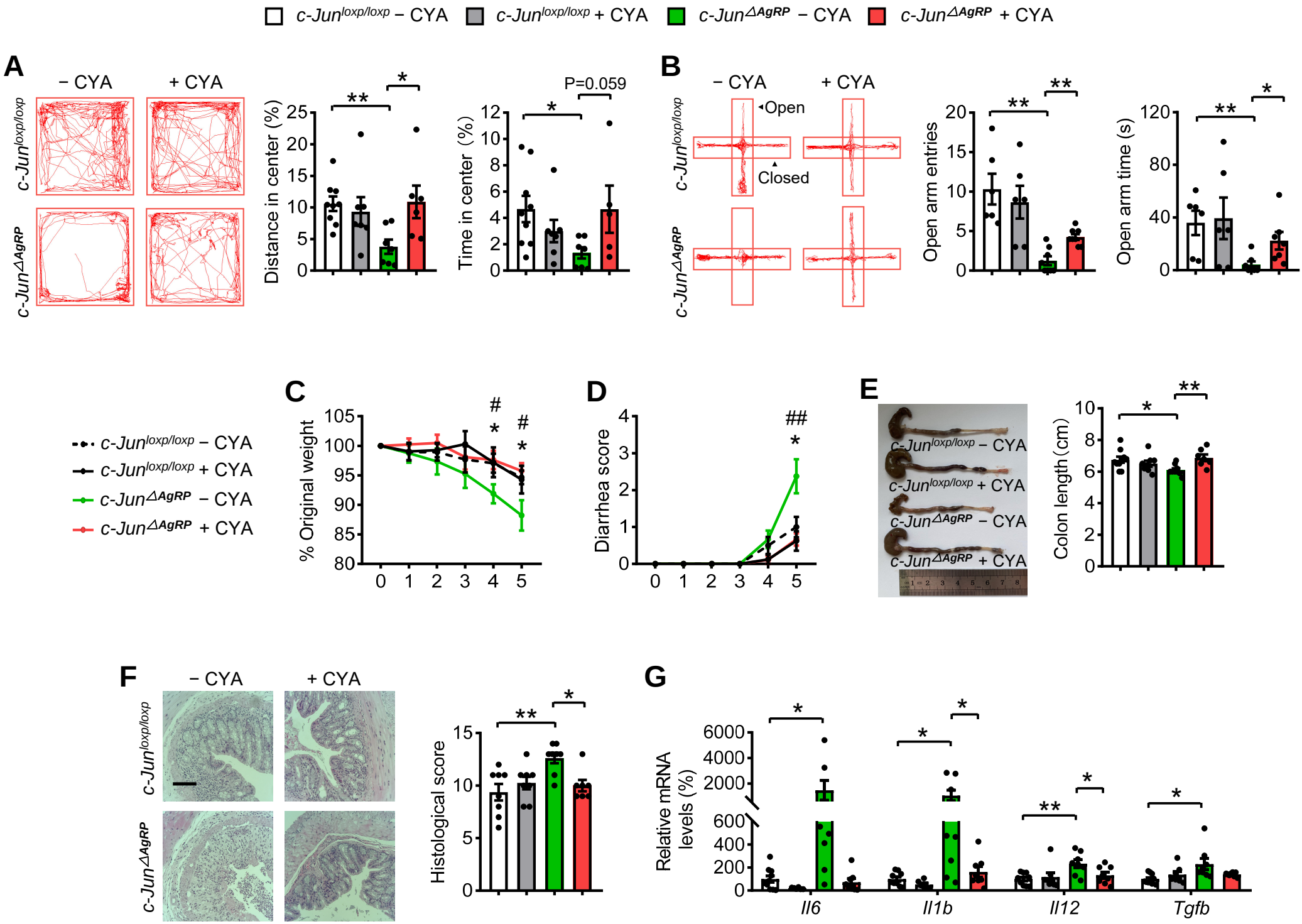
c-Jun loxp/loxp − CYA
c-Jun loxp/loxp + CYA
c-Jun ΔAgRP − CYA
c-Jun ΔAgRP + CYA
A
− CYA
+ CYA
c-Jun loxp/loxp
c-Jun ΔAgRP
Distance in center (%)
Time in center (%)
P=0.059
B
Open
Closed
Open arm entries
Open arm time (s)
C
% Original weight
D
Diarrhea score
E
Colon length (cm)
F
Histological score
G
Relative mRNA levels (%)
Il6
Il1b
Il12
Tgfb

Figure 5

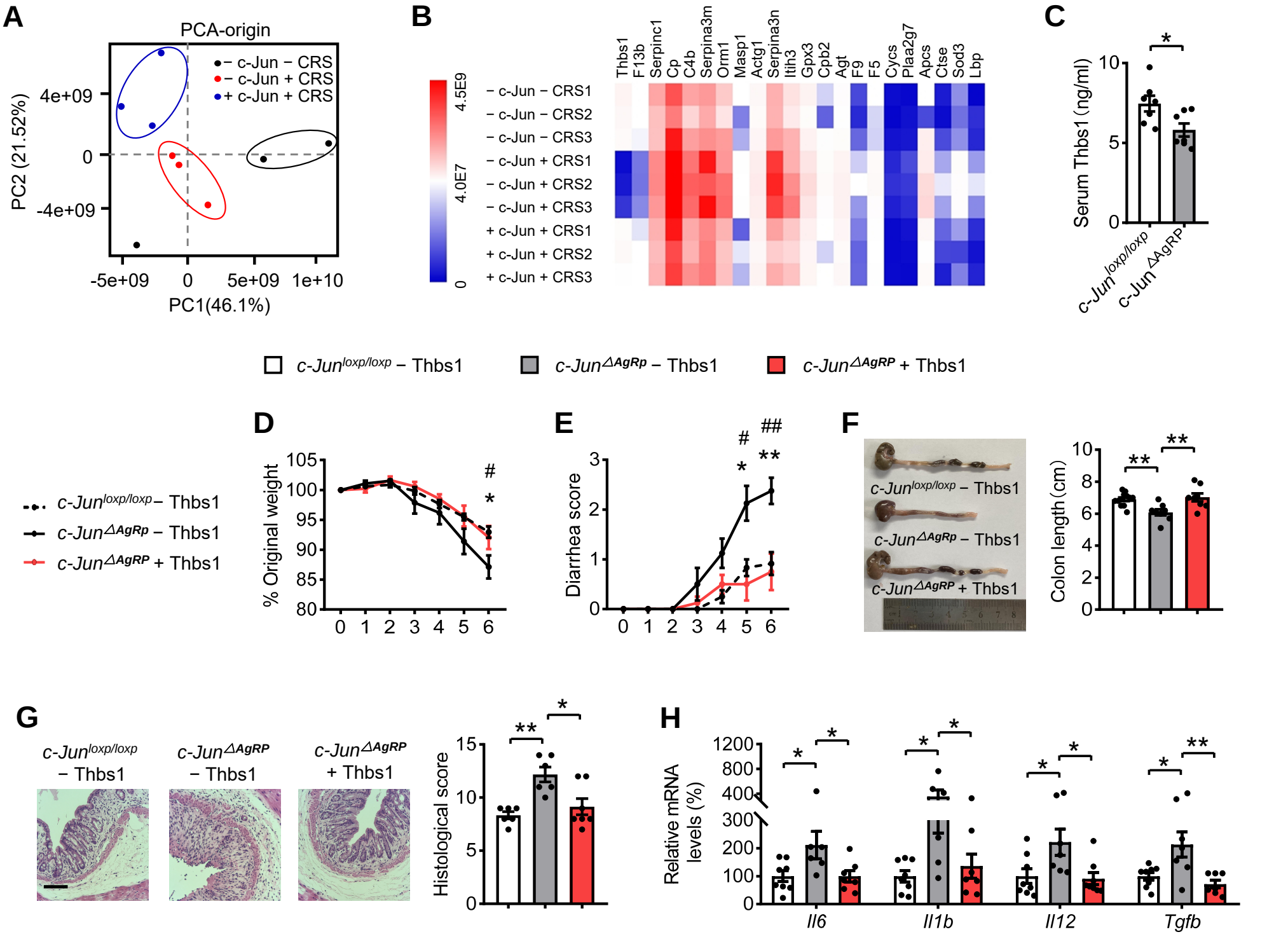
A
PCA-origin
− c-Jun − CRS
− c-Jun + CRS
+ c-Jun + CRS
PC2 (21.52%)
PC1(46.1%)
B
Thbs1
F13b
Serpinc1
Cp
C4b
Serpina3m
Orm1
Masp1
Actg1
Serpina3n
Itih3
Gpx3
Cpb2
Agt
F9
F5
Cycs
Plaa2g7
Apcs
Ctse
Sod3
Lbp
− c-Jun − CRS1
− c-Jun − CRS2
− c-Jun − CRS3
− c-Jun + CRS1
− c-Jun + CRS2
− c-Jun + CRS3
+ c-Jun + CRS1
+ c-Jun + CRS2
+ c-Jun + CRS3
C
Serum Thbs1 (ng/ml)
c-Jun loxp/loxp
c-Jun ΔAgRP
c-Jun loxp/loxp − Thbs1
c-Jun ΔAgRp − Thbs1
c-Jun ΔAgRP + Thbs1
D
% Original weight
E
Diarrhea score
F
Colon length (cm)
G
Histological score
H
Relative mRNA levels (%)
Il6
Il1b
Il12
Tgfb

I

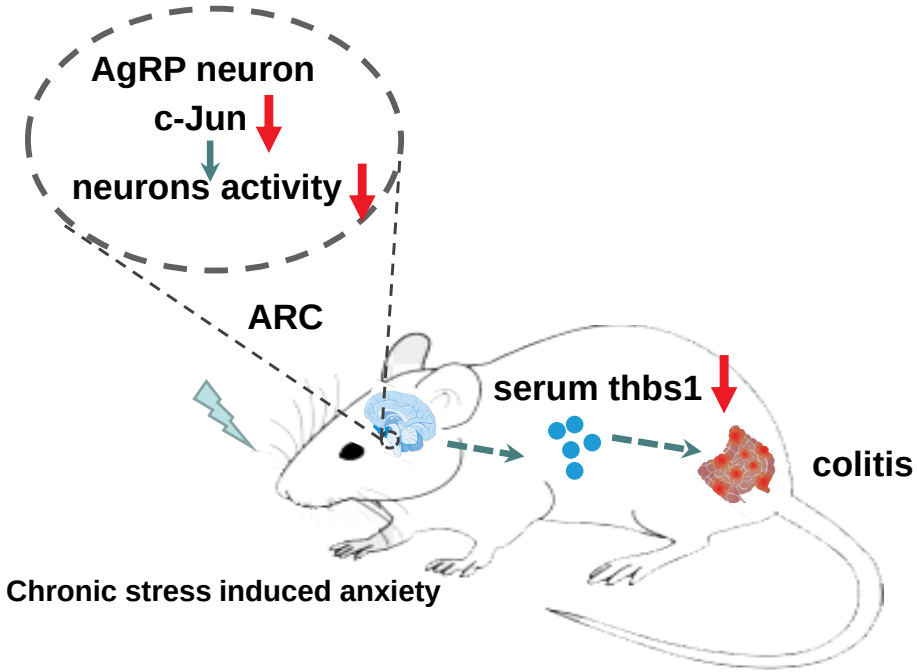
AgRP neuron
c-Jun
neurons activity
ARC
serum thbs1
colitis
Chronic stress induced anxiety

Supplementary Figures and Figure Legends

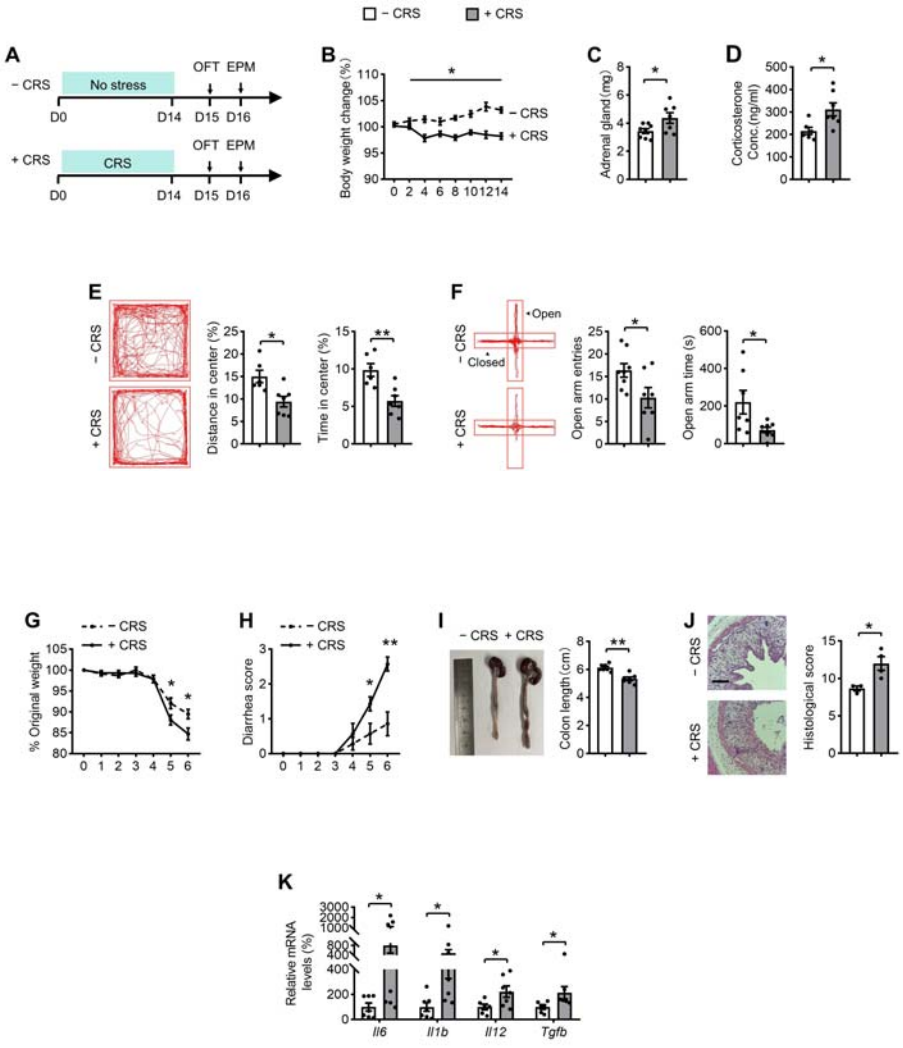

Supplementary Figure 1. Chronic restraint stress (CRS) induces anxiety-like behaviors and increases the susceptibility to colitis. (A) Schematic showing the CRS experimental protocol. (B) Changes of body weight. (C) Adrenal gland weights. (D) Serum corticosterone levels. (E) Representative tracks and statistical results in OF test. (F) Representative tracks and statistics in EPM test. (G) Percentage of body weight loss. (H) Scores of diarrhea. (I) Gross morphology and length of the colon. (J) H&E staining and histological scores of the colon tissues. Scale bar, 110 μm. (K) qRT-PCR

analysis of mRNA expression of inflammatory cytokines (*Il6, Il1b, Il12,* and *Tgfb*) in the distal colon tissues. Studies for A-F were conducted using 12-week-old WT mice with unstress (- CRS) or stressed (+ CRS) treatment for 14 days. Behavioral tests were performed on day 15 (E) and day 16 (F). G-K were conducted using - CRS mice and + CRS mice with 3% DSS in drinking water for 6 days to induce acute colitis; Values are expressed as means ± SEM (n = 3–8 per group), with individual data points. Data were analyzed using two-tailed unpaired Student's *t* test.

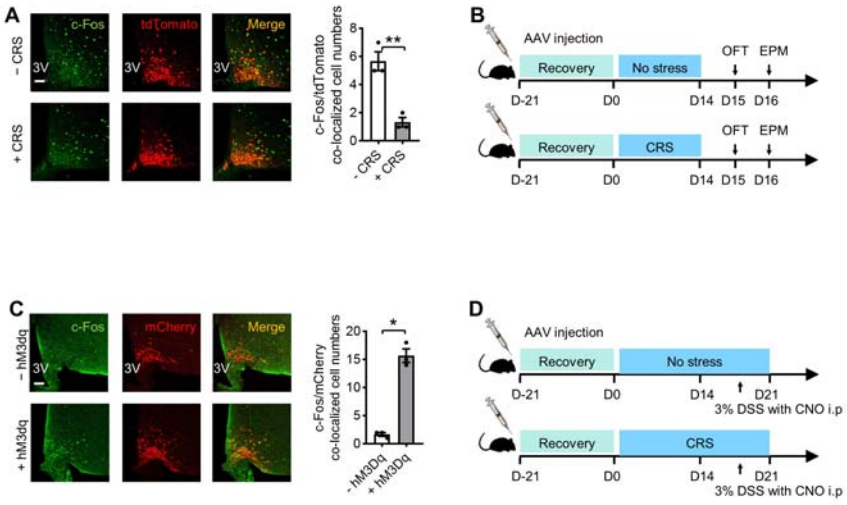

Supplementary Figure 2. Parameters related to mice with activation of AgRP neuronal activity. (A) Immunofluorescence (IF) staining for tdTomato (red), c-Fos (green), and merge (yellow) in the ARC sections (left), and quantification of c-Fos and tdTomato co-localized cell numbers (right). Scale bar, 50 μm. c-Fos staining was coupled with a TSA Plus Fluorescein KIT. (B) Experimental timeline for CRS. (C) IF staining for mCherry (red), c-Fos (green) and merge (yellow) in ARC sections (left), and quantification of c-Fos and mCherry colocalized cell numbers (right). (D) Experimental timeline for DSS administration. Study for A was conducted using

14-week-old AgRP-Cre-Ai9 mice with (+ CRS) or without (- CRS) 14 days of stress. C was conducted using 10- to 12-week-old AgRP-Cre mice receiving AAV expressing mCherry (- hM3Dq) or hM3Dq (+ hM3Dq), both treated with one injection of CNO and 30 min later for immunofluorescence analysis. Values are expressed as means ± SEM (n = 3-4 per group), with individual data points. Data were analyzed using two-tailed unpaired Student's *t* test.

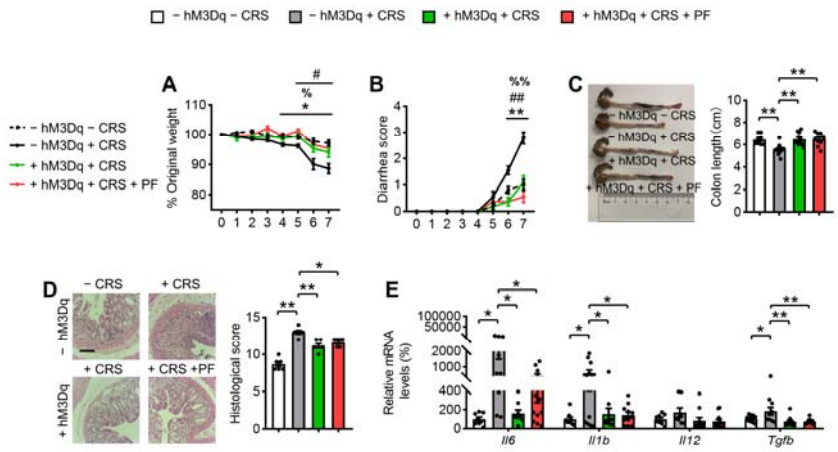

Supplementary Figure 3 Pair-feeding has no beneficial effect on the improvement of colitis. (A) Percentage of body weight loss. (B) Scores of diarrhea. (C) Gross morphology and length of the colon. (D) H&E staining and histological scores of the colon tissues. Scale bar, 110 μm. (E) qRT-PCR analysis of mRNA expression of inflammatory cytokines (*Il16, Il1b, Il12,* and *Tgfb*) in the distal colonic tissues. Studies were conducted using 10- to 12-week-old AgRP-Cre mice receiving AAV expressing mCherry (- hM3Dq) or hM3Dq (+ hM3Dq), all mice experienced unstressed (- CRS) or stressed (+ CRS) treatment for 14 days, after that was under

treatment of 3% DSS in drinking water for 7 days to induce acute colitis, simultaneously receiving CNO injections every 12 hours per day. Pair-fed (PF) experiment was administered during CNO injection. For pair-fed groups (+ hM3Dq + CRS + PF), mice were given the same diet as the - hM3Dq + CRS groups. Values are expressed as means ± SEM (n=6-11 per group), with individual data points. Data were analyzed using two-way ANOVA, followed by Tukey's multiple comparisons test. - hM3Dq + CRS versus - hM3Dq – CRS, *P <0.05, **P <0.01; + hM3Dq + CRS versus - hM3Dq + CRS, $^{\#}$P <0.05, $^{\#\#}$P <0.01; + hM3Dq + CRS + PF versus - hM3Dq + CRS, $^{\%}$P <0.05, $^{\%\%}$P <0.01 (A-B).

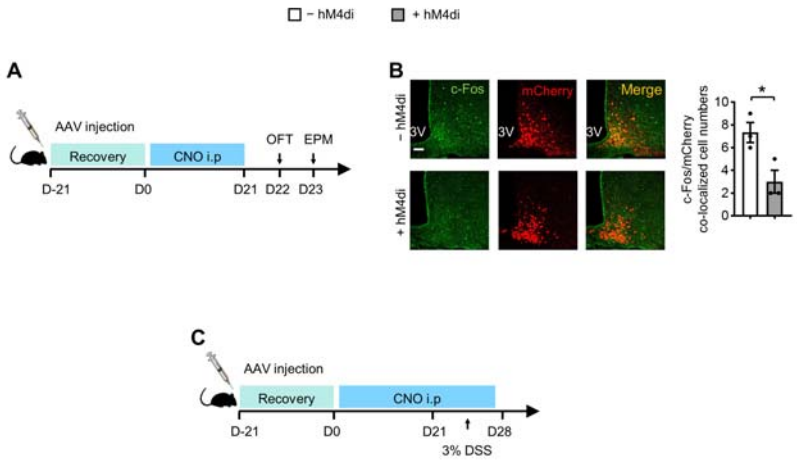

Supplementary Figure 4. Parameters related to mice with inhibition of AgRP neuronal activity. (A) Experimental timeline for CRS. (B) Immunofluorescence (IF) staining for mCherry (red), c-Fos (green) and merge (yellow) in ARC sections (left), and quantification of c-Fos and mCherry colocalized cell numbers (right). (C) Experimental timeline for DSS administration. Study for B was conducted using 10- to 12-week-old AgRP-Cre mice receiving AAV expressing mCherry (- hM4Di) or

hM4Di (+ hM4Di) both treated with one injection of CNO and 30 min later for immunofluorescence analysis. Values are expressed as means ± SEM (n = 3 per group), with individual data points. Data were analyzed using two-tailed unpaired Student's *t* test.

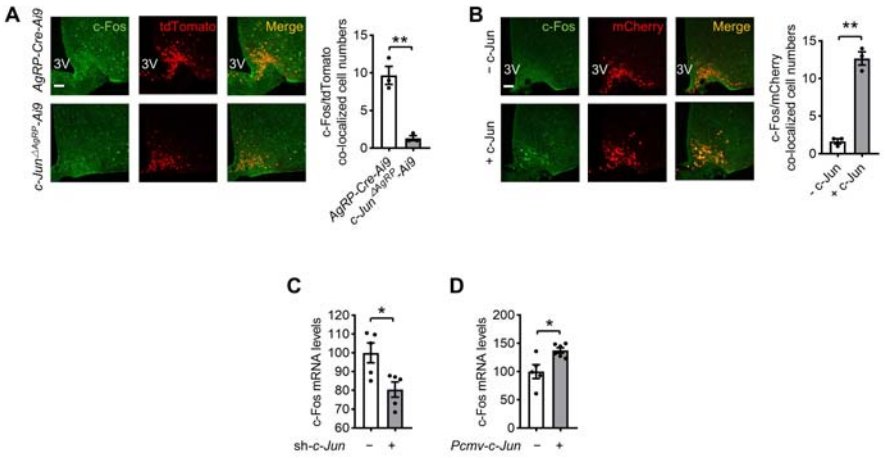

Supplementary Figure 5. The changes of c-Fos after c-Jun deletion and overexpression in vitro and in vivo. (A) IF staining for tdTomato (red), c-Fos (green) and merge (yellow) in ARC sections (left), and quantification of c-Fos and tdTomato colocalized cell numbers (right). (B) IF staining for mCherry (red), c-Fos (green) and merge (yellow) in ARC sections (left), and quantification of c-Fos and mCherry colocalized cell numbers (right). (C-D) C-Fos mRNA levels. Study for A was conducted by mating Ai9 (tdTomato) mice with AgRP-irs-Cre mice to obtain AgRP-Ai9 mice as controls, mating Ai9 (tdTomato) mice with mice with c-Jun deletion in AgRP neurons (*c-Jun*$^{\Delta AgRP}$) to obtain *c-Jun*$^{\Delta AgRP}$-Ai9 mice. B was conducted using 12- to 14-week-old AgRP-Cre mice receiving AAV expressing mCherry (- c-Jun) or c-Jun (+ c-Jun). C was conducted on primary hypothalamus

isolated from newborn mice, receiving control (-sh-*cJun*) or sh-*cJun* (+ sh-cJun) transfected with Lipo 3000. D was conducted on primary hypothalamus isolated from newborn mice, receiving control (- pcmv-*c-Jun*) or c-Jun (+ pcmv-*c-Jun*) transfected with Lipo 3000. Values are expressed as means ± SEM (n=3-6 per group), with individual data points. Data were analyzed using two-tailed unpaired Student's *t* test.

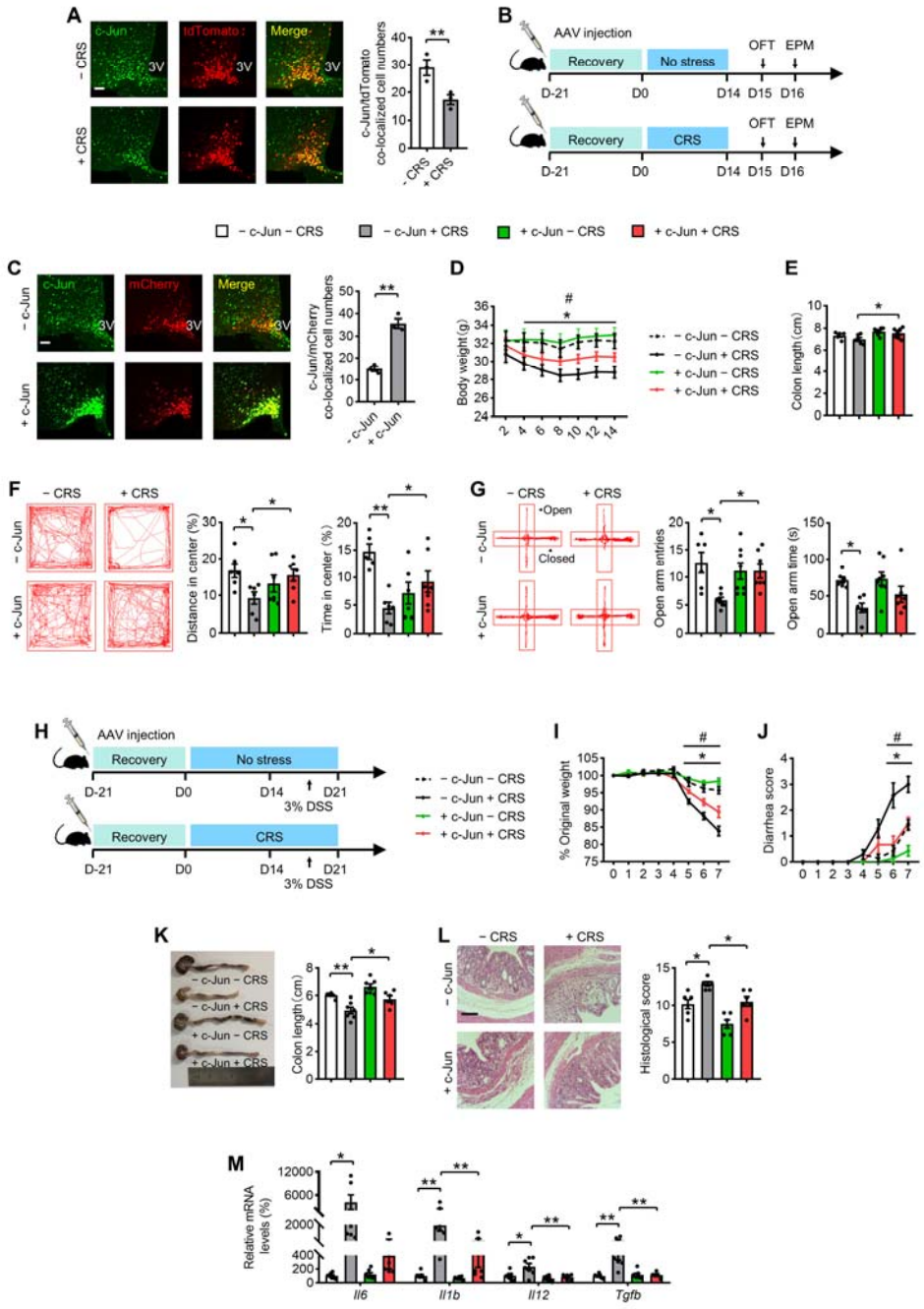

Supplementary Figure 6. Overexpression of c-Jun in AgRP neurons leads to resistance to CRS-induced anxiety-like behaviors and colitis. (A) IF staining for tdTomato (red), c-Jun (green) and merge (yellow) in ARC sections (left), and quantification of c-Jun and tdTomato colocalized cell numbers (right). (B) Experimental timeline for CRS. (C) IF staining for mCherry (red), c-Jun (green) and merge (yellow) in ARC sections (left), and quantification of c-Jun and mCherry colocalized cell numbers (right). (D) Body weight. (E) Colon length. (F) Representative tracks and statistical results in OF test. (G) Representative tracks and statistics in EPM test. (H) Experimental timeline for DSS administration. (I) Percentage of body weight loss. (J) Scores of diarrhea. (K) Gross morphology and length of the colon. (L) H&E staining and histological scores of the colon tissues. Scale bar, 110 μm. (M) qRT-PCR analysis of mRNA expression of inflammatory cytokines (*Il16, Il1b, Il12,* and *Tgfb*) in the distal colonic tissues. Study for A was conducted using 14-week-old AgRP-Cre-Ai9 mice with (+ CRS) or without (- CRS) 14 days of stress. C was conducted using 12- to 14-week-old AgRP-Cre mice receiving AAV expressing mCherry (- c-Jun) or c-Jun (+ c-Jun), IF staining performed after 3 weeks from AAV recovery. D-G were conducted using – c-Jun mice and + c-Jun mice, both experienced unstressed (- CRS) or stressed (+ CRS) treatment for 14 days. Behavioral tests were performed on day 15 (F) and day 16 (G). H-M were conducted using - c-Jun mice and + c-Jun mice receiving 3% DSS in drinking water for 7 days to induce acute colitis, after stress (+ CRS) or unstress (- CRS). Values are expressed as means ± SEM (n=3-8 per group), with individual data points. Data were

analyzed using two-tailed unpaired Student's *t* test (A, C). Data were analyzed using two-way ANOVA, followed by Tukey's multiple comparisons test (D-M). - c-Jun + CRS versus - c-Jun - CRS *P <0.05, **P <0.01. + c-Jun + CRS versus - c-Jun + CRS, $^{\#}$P <0.05, $^{\#\#}$P <0.01 (D, I-J).

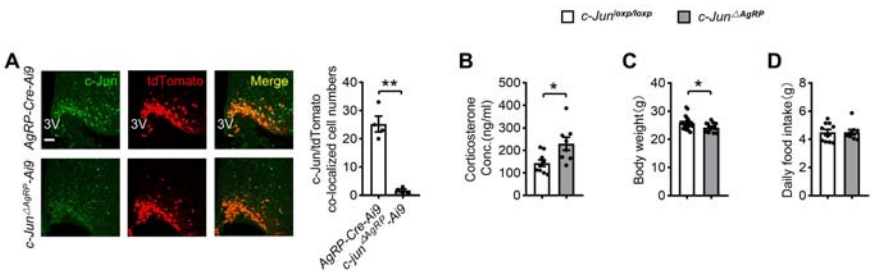

Supplementary Figure 7. Biochemical parameters related to *c-Jun*$^{\Delta AgRP}$ mice. (A) IF staining of tdTomato (red), c-Jun (green) and merge (yellow) in ARC sections (left), and quantification of c-Jun and tdTomato colocalized cell numbers (right). (B) Serum corticosterone levels. (C) Body weight. (D) Food intake. Study for A was conducted using AgRP-Cre-Ai9 mice and *c-Jun*$^{\Delta AgRP}$-Ai9 mice. B-D were conducted using c-*Jun*$^{loxp/loxp}$ mice or *c-Jun*$^{\Delta AgRP}$ mice. Values are expressed as means ± SEM (n=4-20 per group), with individual data points. Data were analyzed using two-tailed unpaired Student's *t* test.

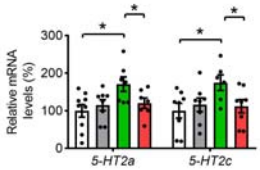

Supplementary Figure 8. The efficacy of anxiolytic drug cyamemazine (CYA).

mRNA levels of 5-HT2a and 5-HT2c. Study was conducted using 18- to 20-week-old *c-Jun*$^{loxp/loxp}$ mice and *c-Jun*$^{\Delta AgRP}$ mice treated with (+ CYA) or without (- CYA) followed by DSS administration. Values are expressed as means ± SEM (n=6-9 per group), with individual data points. Data were analyzed using two-way ANOVA, followed by Tukey's multiple comparisons test.

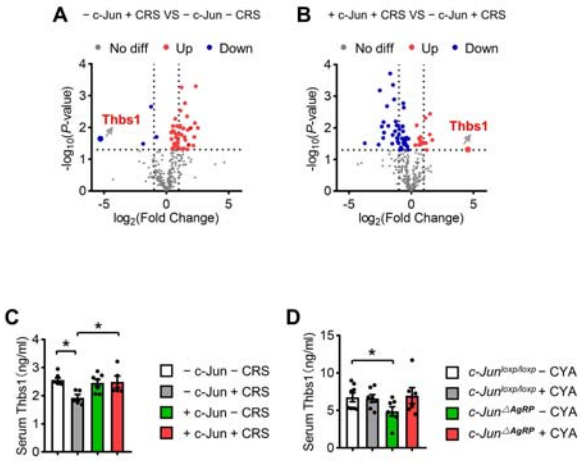

Supplementary Figure 9. Parameters related to *c-Jun*$^{\Delta AgRP}$ mice with thbs1 supplementary. (A) Volcano plot of detected proteins between - c-Jun + CRS mice and - c-Jun - CRS after DSS insults; THBS1 is indicated. (B) Volcano plot of detected proteins between + c-Jun + CRS and - c-Jun + CRS after DSS insults; THBS1 is indicated. (C-D) Serum thbs1 levels. Studies for A-B were conducted using - c-Jun - CRS mice, - c-Jun + CRS mice and + c-Jun + CRS mice to analyze of serum secreted proteins. C was conducted using - c-Jun mice and + c-Jun mice receiving 3% DSS in drinking water for 7 days to induce acute colitis, after stress (+ CRS) or unstress (-

CRS). D was conducted using *c-Jun*$^{loxp/loxp}$ and *c-Jun*$^{\Delta AgRP}$ mice administrated with 3% DSS for 5 days to induce acute colitis with (+ CYA) or without (- CYA) CYA. Values are expressed as means ± SEM (n=3-7 per group), with individual data points. Data were analyzed using two-tailed unpaired Student's *t* test (A-B). Data were analyzed using two-way ANOVA, followed by Tukey's multiple comparisons test (C-D).